

Physical Constraints on Marine Osmotrophy in an Optimal Foraging Context ¹

Peter A. JUMARS ², Jody W. DEMING², Paul S. HILL ^{2,3},
Lee KARP-BOSS ², Patricia L. YAGER ²
and W. Brian DADE^{2,4}

² *School of Oceanography, WB-10, University of Washington, Seattle, WA 98195, USA.*

³ *Department of Oceanography, Dalhousie University, Halifax, NS B3H 4J1, Canada.*

⁴ *Department of Applied Mathematics and Theoretical Physics, University of Cambridge, 20 Silver Street, Cambridge CB3 9EW, England*

Abstract

Unattached, heterotrophic osmotrophs the size of typical free-living, water-column bacteria have no means to enhance steady-state diffusive fluxes of nutrients toward themselves beyond $4\pi r_0 DC_\infty$ mol cell⁻¹ time⁻¹, where r_0 is the cell radius [L], D is the diffusion coefficient for the nutrient [L² T⁻¹] and C_∞ is ambient concentration of the nutrient [mol L⁻³]. Altering cell size (r_0) does allow maximization of net gain because this gain function is linear in cell radius while the rate at which nutrients are used is not. If one assumes that utilization rates of nutrients in growth and catabolism scale as r_0^a , where $1 < a < 3$, there is an optimal cell size that increases with C_∞ . Temperature affects diffusive flux through its effect on D , yielding a Q_{10} of about 1.2 to 1.4 for growth rates that are diffusion limited. Over a large range of growth temperatures spanning the one (T_a) to which a culture is adapted, however, it is likely that diffusional limitation will occur at the highest temperatures and reaction-rate limitation will occur below T_a . As temperature is lowered, reactions with higher Q_{10} will tend to become limiting. Hence nonlinearity is to be expected in Arrhenius plots of cell growth rate. Photoautotrophs have the obvious advantage of independence from diffusion in securing their energy (but not their mass) and also may be large enough to gain relative diffusional advantage at high turbulence intensities; gross gain then rises faster than linearly with increasing size, steeply increasing optimal size. We find that extant predictive equations for Sherwood number (ratio of mass transfer across the surface of a sphere relative to mass transfer in stagnant fluid) — with slight modifications to make them consistent with the Sherwood-number definition and with each other — fit extant data for the Péclet number region from 1-100, obviating the need for interpolating functions. Bacterivores that utilize ambient flow to effect direct interception of bacteria also gain from enhanced fluid shear, and bacterivores that feed by Brownian motion of their prey gain from it

¹ Supported by Office of Naval Research Grant N00014-90-J-1078.

analogously with large phytoplankton. Thus under steady conditions ($\partial C/\partial t = 0$, where C is the concentration of food molecules or particles), moderate to high levels of shear favor the larger osmotrophic competitors and the predators of bacteria over bacteria themselves.

The distributed (in space and time) nature of nutrient sources for bacteria, coupled with fluid shear from turbulent dissipation, makes their nutrient environment in oligotrophic waters much more extremely time varying, however, than the milieu of batch or chemostat cultures. We suggest that the periplasm and perhaps the capsule constitute a nutrient reservoir that is filled in episodic encounters with high concentrations and then utilized during subsequent scarcity. This strategy would allow the cell using it to have the same long-term average nutrient uptake rate with fewer transporters than would be required by a cell without such a buffer. Queueing theory as applied to the transient condition holds promise for analyzing the buffering capacity of this reservoir and its contribution to short-term and long-term growth.

Key words: Osmotrophs, Diffusion, Temperature, Turbulence.

Résumé

Contraintes physiques sur l'osmotrophie marine dans un contexte de nutrition optimale

Les osmotrophes hétérotrophes non fixés à un substrat, de la taille des bactéries libres de la pleine eau, n'ont aucune possibilité d'accroître les flux de nutriments, par diffusion, à destination de leurs cellules au-delà de $4\pi r_0 D C_\infty$ molécules par cellule et pour un temps donné, avec r_0 , le rayon de la cellule [L], D le coefficient de diffusion pour le nutriment [$L^2 T^{-1}$] et C_∞ la concentration ambiante du nutriment [$mol L^{-3}$]. La variation de la taille de la cellule (r_0) permet de maximiser le gain net parce que cette fonction de gain est linéaire pour le rayon de la cellule tandis que le taux auquel le nutriment est utilisé ne l'est pas. Si on suppose que les taux d'utilisation des nutriments dans la croissance et le catabolisme varient comme r_0^a , avec $1 < a < 3$, il existe une taille optimale de la cellule qui augmente avec C_∞ . La température affecte le flux par diffusion par l'intermédiaire de son effet sur D , donnant un Q_{10} d'environ 1,2 à 1,4 pour les taux de croissance qui sont limités par la diffusion. Pour une grande gamme de températures de croissance comprenant la température (T_a) à laquelle la culture est adaptée, cependant, il est vraisemblable que la limitation due à la diffusion se produira aux plus hautes températures et que la limitation liée à la vitesse de réaction aura lieu au dessous de T_a . Lorsque la température est abaissée, les réactions possédant les Q_{10} les plus élevés tendront à devenir limitantes. Pour cette raison une non-linéarité doit être attendue dans les diagrammes d'Arrhenius de la croissance cellulaire. Les photoautotrophes ont l'avantage évident d'être indépendants de la diffusion pour obtenir leur énergie (mais non leur masse) et peuvent ainsi être assez grands pour obtenir un avantage relatif en ce qui concerne la diffusion, aux turbulences élevées; le gain brut alors s'élève plus vite que linéairement avec l'augmentation de taille, faisant monter en flèche la dimension optimale. Nous trouvons que les équations prédictives existant pour le nombre de Sherwood (rapport du transfert de masse au travers de la surface d'une sphère au transfert de masse dans un fluide stagnant) — avec de légères modifications pour les rendre compatibles avec la définition du nombre de Sherwood et entre elles — s'accordent avec les données existantes pour la zone du nombre de Péclet allant de 1 à 100, sans qu'il soit besoin de fonctions d'interpolation. Les bactérivores qui utilisent le flux ambiant pour effectuer l'interception directe des bactéries bénéficient aussi d'un cisaillement accru du fluide, et les bactérivores qui se nourrissent grâce au mouvement brownien de leurs proies en bénéficient de façon analogue avec le grand phytoplancton. Ainsi sous des conditions constantes ($\partial C/\partial t = 0$, où C est la concentration des molécules ou des particules nutritives), des niveaux modérés à élevés de cisaillement favorisent les plus grands compétiteurs osmotrophes et les prédateurs de bactéries par rapport aux bactéries elles mêmes.

La nature de la distribution (dans l'espace et dans le temps) des sources nutritives des bactéries, couplée avec le cisaillement du fluide provenant de la dissipation turbulente, fait leur environnement nutritif dans les eaux oligotrophes extrêmement variable dans le temps, beaucoup plus que dans le milieu des cultures ou du chimostat. Nous suggérons que le périplasme, et peut-être la capsule, constitue un réservoir nutritif qui est rempli lors des rencontres épisodiques avec les hautes concentrations et utilisé ensuite durant les périodes de

disette qui suivent. Cette stratégie permettrait à la cellule qui l'emploie d'avoir le même taux d'absorption moyen du nutriment sur le long terme avec moins de transporteurs que ne le demanderait une cellule dépourvue d'un tel tampon. La théorie de la queue appliquée aux conditions transitoires est prometteuse pour analyser la capacité de tampon de ce réservoir et sa contribution à la croissance sur le court terme et le long terme.

Introduction

At low temperatures, bacteria appear to be at a disadvantage relative to photoautotrophs in particular (Pomeroy and Deibel, 1986; Pomeroy *et al.*, 1990) and to other organisms in general (Larsson and Hagström, 1982; Hagström and Larsson, 1984; Scavia and Laird, 1987; Wikner and Hagström, 1991). Among the few specific, published mechanisms that we can find to explain low-temperature disfunction in aquatic bacteria is the suggestion by Haight and Morita (1966) that glycolytic enzyme levels or perhaps membrane permeability decrease in cells grown at low temperature, though it is not plain why bacteria should suffer such apparent disadvantages disproportionately to other taxa, nor is it clear that other bacterial strains beyond the one studied by Haight and Morita (1966) would show similar responses. Weakening of hydrophobic bonds and strong feedbacks in enzyme regulation are documented effects of low temperature on better-known (*i.e.* non-marine) bacteria and have been shown to account for steep reduction in growth rates as temperatures fall (Neidhardt *et al.*, 1990), but again it is not apparent that bacteria should experience such effects any more severely than do other poikilotherms, and few — if any — extreme psychrophiles have yet been studied from this perspective (Deming, 1993; Yager, in prep.).

To recapitulate what is and is not known about thermal regulation on the basis of the data cited above, it is worth drawing parallels with recent advances in understanding of the regulation of phytoplankton populations in the sea. Where seasonal events, *i.e.* deep mixing, uncouple populations of phytoplankton from their grazers, seasonal phytoplankton blooms are anticipated and observed (Evans and Parslow, 1985); annual cycles in nutrient supplies and insolation lead phytoplankton blooms in phase. In the case of photoautotrophs, these nutrients are inorganic and are not in short supply at the outset of a bloom. At least for their energy supplies, however, heterotrophic bacteria depend upon organic nutrients. There are two major pathways of organic nutrients to bacteria (Pomeroy, 1974), a direct one from exudates and particulate remains of phytoplankton that go uneaten by eukaryotes and an indirect one from phytoplankton and higher trophic levels via by-products of feeding activity. No matter the pathway, the seasonal cycle of phytoplankton abundance and production in these environments where food-web connections are uncoupled by the lack of net primary production in winter must lead the bacterial cycle in phase. Temperature and light cycles therefore must lead both phytoplankton and bacterial cycles of abundance and production. It thus is impossible from field observations alone to disentangle regulation of bacterial growth by temperature versus by organic nutrient supply. Community-level

temperature manipulations with nutrient levels left at their field levels, such as those carried out by Pomeroy and Deibel (1986), also leave temperature and food confounded as regulators of bacterial growth, prompting Pomeroy *et al.* (1990, 1991) to pursue parallel field and laboratory experiments to distinguish these effects. In the meantime, to conclude from seasonal observations in the field that temperature *per se* regulates bacterial growth is analogous to concluding from the timing of weight gain that growth of livestock in the spring is light or temperature limited.

Absolute comparison of low-temperature performance in photoautotrophs versus heterotrophic osmotrophs may be neither desirable nor possible: it is not clear what light regime and concentrations of inorganic and organic nutrients would allow a "fair" contest. Rather, our purpose is to examine each of the physical factors, including cell size, that determine the rates of arrival of nutrient molecules at cell membranes of planktonic osmotrophs. Because the relevant literature is widely scattered and because on some issues data and theory agree poorly, a major function of our paper is to provide the reader with easy access to simple, explicit equations (both theoretical and empirical) to calculate physical effects on nutrient fluxes under conditions beyond the limited suite that we can explore here. We search this small set of physical and chemical factors for clues as to disadvantage of bacteria with respect both to eukaryotic osmotrophs and to bacterivores at low temperatures before and during phytoplankton blooms at high latitudes. Our search focuses on physical and chemical factors external to the bacterial cell membrane because *a priori* we perceive no obvious biological or biochemical mechanism for inferior physiological performance of bacteria at low temperatures or high latitudes. To support our goal of giving broad access to calculations, we include primary dimensions of variables in brackets [$M^a L^b T^c$], where M stands for mass, L for length and T for time and the lower-case letters indicate specific exponents for the problem under consideration. Because they are still most common, we use cgs units in our explicit calculations, though we provide SI equivalents where they are also commonly used (*Appendix*).

To provide a different perspective from that presented in prior reviews of bacterial osmotrophy, we adopt the viewpoint of optimal foraging theory (Stephens and Krebs, 1986), *i.e.* that an individual osmotroph acting to maximize its average net rate of gain of nutrients will enjoy greater fitness. We go from unrealistic, simple planktonic environments to more realistic and complex planktonic ones to fulfill our goal of making the calculations accessible — to show how the calculations must change with successive complications. We do so as well because common laboratory environments may fall closer to the simple, unrealistic end of the spectrum than heretofore appreciated.

Of the three major bacterial environments in the sea (Table I), we treat primarily the free-living planktonic one. Bacteria in the plankton are sparse enough that their diffusional spheres of influence on average do not overlap. Fluid motion continually rearranges spatial relationships, making it difficult or impossible to modify a local environment to the benefit of clone members. Hence it is reasonable to evaluate fitness in terms of individual gain. Even if phage transduction transfers adaptations laterally, they are still selected within the context of individual success. This conclusion of

TABLE I. – Characteristics of principal marine environments of bacteria. The table is an expansion of the graphical arguments of Plante *et al.* (1990, their Fig. 2).

<i>Environment</i>	<i>Gain to an individual from its free release of exoenzymes</i>	<i>Gain to clone mates from free release of exoenzymes</i>	<i>Stability of association with neighbors</i>	<i>Selection operates on</i>	<i>Sherwood number^a</i>	<i>Efficacy of chemokinesis</i>
Planktonic, free living	Negligible	Negligible except in dense, monospecific blooms	Low	Individuals	$\cong 1$	Low (disrupted by shear)
Oxic, attached (suspended particles or oxic sediments)	Moderate	Negligible to moderate	Moderate	Individuals and local clone members	≥ 1	High (strong, stable gradients in pore fluids)
Anoxic, enclosed (sediments or gut contents)	High	High	High	Individuals, local clone members and consortia	$\cong 1$ in sediments or ≥ 1 in guts	Low in sediments (Pore spaces poorly connected)

^a A measure of the relative magnitude of mass transfer by fluid advection versus molecular diffusion; see text.

selection at the level of the individual may be invalid for plankton of smaller freshwater bodies or marine tide pools that are not treated here. It may also be invalid for occasional, dense, monospecific blooms in the sea. Among bacteria on large particles in the water column or in the oxic seabed, spatial relationships are maintained longer, and it is far more likely that clone members and other neighbors interact, complicating the evaluation of fitness considerably. In enclosures, the likelihood of significant intra- and inter-clone interaction increases markedly, since the probability that molecules released by one individual will interact with other bacteria in the enclosure is high (*cf.* the arguments of Plante *et al.*, 1990, their Fig. 2), and the action of the group can modify the ambient chemical environment. Because of biological activity, such enclosures usually are anoxic. Fitness outside the free-living plankton may well be maximized by behaviors other than those that yield maximal net rates of gain to an individual.

To build toward calculations for the typical planktonic situation, we go through two simpler intermediates. Specifically, we treat a homogeneous environment in the absence of fluid motion first, then add fluid motion in the absence of chemical heterogeneity and finally add chemical heterogeneity in the presence of fluid motion. The primary purpose of this structure is to allow the derivations to be followed, reproduced and criticized as easily as possible. The simpler cases do apply, however, in limited settings and so are useful in themselves. Even in the simplest case of food supply by molecular diffusion alone, some aspects deserve more attention in the light of foraging theory.

We thank Frank Millero, University of Miami, and Eric O. Hartwig, Naval Research Laboratory, for confirming the lack of published experimental work on dynamic viscosity of seawater below 0°C. We thank three anonymous reviewers for their constructive comments on an earlier draft and Arthur Nowell and Jeff Shimeta for useful discussions.

Cells in a stagnant, homogeneous ocean

Cell size at constant temperature

Prevailing thinking is that smaller bacteria are more efficient at extracting nutrients. The quantitative accuracy of this idea depends upon the definition that one chooses for efficiency (E). The most widely adopted parameterization in bacterial physiology and ecology is that of Koch (1971, 1985, 1990):

$$E = \frac{\text{Volume of solution cleared of solute time}^{-1}}{\text{Volume of cell}} \quad (1)$$

Koch further showed that in the absence of advective fluid motion, when only molecular diffusion acts, there is a physically imposed upper limit on this efficiency

(E_{max}) that varies with cell radius (r_0) and the solute's molecular diffusion coefficient (D):

$$E_{max} = \frac{3D}{r_0^2} \quad (2)$$

This choice of parameters facilitates comparison with data, since E can be estimated in culture and compared with calculated E_{max} (Koch and Wang, 1982), but it leads to thinking that smaller is always better and thus fails to explain the common observation that cells grown under more eutrophic conditions either in the field or in the laboratory tend to be larger. E also is somewhat counterintuitive in its units [T^{-1}]. In the parlance of aquatic ecology, it is a specific clearance rate rather than an efficiency. Furthermore, efficiencies of nutrient gain versus rates of nutrient gain as foci often lead to divergent conclusions concerning optimality (*e.g.* Shimeta and Jumars, 1991). We suggest, in keeping with the logic of optimal foraging theory (Stephens and Krebs, 1986), that a focus on net rates of gain is usually the more informative regarding fitness. The cell has no means to detect volume cleared (or, for that matter, ambient concentration of nutrient in the medium or D), but certainly does respond to absolute flux arriving at the cell surface (J).

Koch (1971) based his definition of efficiency on the equation for diffusion in spherical coordinates:

$$\frac{\partial C}{\partial t} = D \frac{1}{r^2} \frac{\partial}{\partial r} \left(r^2 \frac{\partial C}{\partial r} \right) \quad (3)$$

The origin of the coordinate system is placed at the center of the cell so that symmetry in the angular coordinates makes all variations a function of radius (r) alone. Steady-state solution of this equation for the flux by molecular diffusion (J_D [$\text{mol cell}^{-1} \text{T}^{-1}$]) of a solute to a spherical cell, where the minus sign indicates flux toward rather than away from the cell is:

$$J_D = -4\pi r_0 D (C_\infty - C_0) \quad (4)$$

Here C is concentration of the nutrient [mol L^{-3}], highest at a large distance from the cell (C_∞) and lowest right at the surface of the cell membrane (C_0). For the moment, assume that the entire surface of the cell is uniformly absorptive, but we will soon relax this assumption. Numerous authors (*e.g.* Koch, 1971; Berg, 1983; Jumars, 1993) have given the intermediate steps for arriving at this analytic solution by repeated integration of Eq. 3. Eq. 4, in turn, is an intermediate step in the derivation of Eq. 2 (Koch, 1971) and in that sense is simpler.

It is important to note that this gross rate of gain by the cell is dependent on its radius, the diffusion coefficient and nutrient concentration at the cell surface, and *not just on ambient concentration far from the cell*. Despite this unassailable fact, most bacterial and algal uptake and growth rates are by convention evaluated as functions of

ambient concentration (C_∞) alone, perform producing scatter due to variations in D , r_0 and C_0 in the relationship between concentration and uptake rate. Unlike the case for more familiar, one-dimensional boundary layers in Cartesian coordinates, there is neither a continuous linear gradient nor an abrupt outer limit to the concentration boundary layer. Rather, when steady state is reached, concentration varies as the inverse of distance from the cell surface (Fig. 1), asymptoting at the ambient concentration. This result is easy to intuit by imagining successive spherical “shells” of increasing radius (r) about the cell; at steady state the flux through each successive shell must be equal. To maintain this constancy (since surface area of the shells increases as r^2), flux per unit of area of the shell must decrease as $1/r^2$, and hence the concentration gradient driving that flux likewise must be inversely proportional to r^2 (Fig. 1).

The influence of physiology is limited to but two parameters in Eq. 4, namely r_0 and C_0 . A cell can increase total gross flux to itself by enhancing its active uptake system

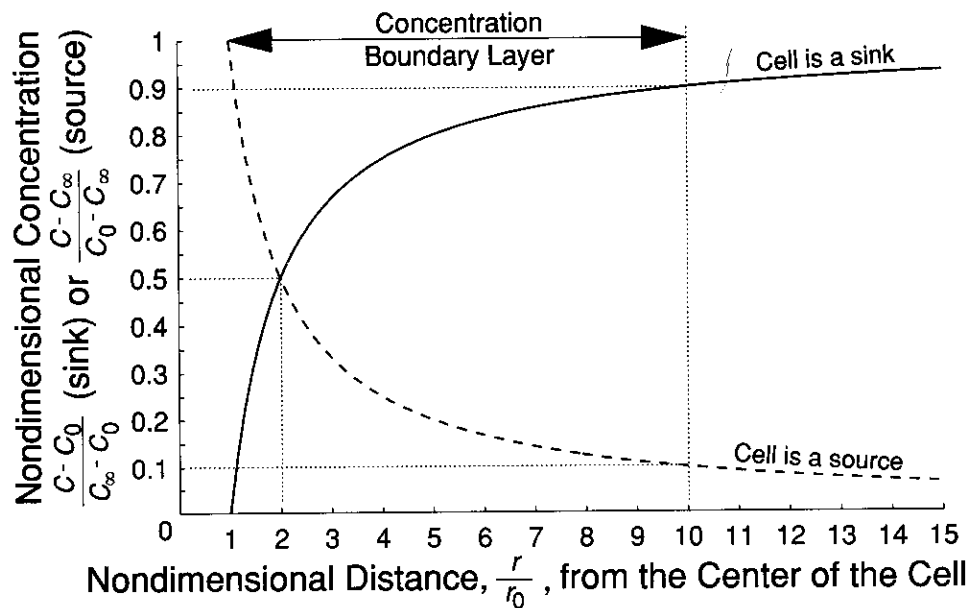


Fig. 1. Concentration (C) of a solute versus distance (r) from the center of a spherical cell when the cell is a sink (solid curve) for the solute or is its source (dashed curve). Subscripts refer to the radial coordinate; ∞ is far from the cell and 0 is at the cell surface, a distance r_0 from the center of the spherical coordinate system. No advective (or convective) motion is assumed. Note that the cell's influence falls substantially by a distance of one cell radius from its surface ($r/r_0 = 2$) and penetrates little beyond a distance of nine cell radii from the outer cell wall ($r/r_0 = 10$). Both axes are given in nondimensional form for generality. While the concentration gradient is steep at the cell surface (r_0) when drawn in this form, it should be remembered that the gradient (dC/dr) that drives diffusion depends on the absolute size of the cell. Throughout the text we refer to the region inside the dotted line at $r/r_0 = 10$ as the “concentration boundary layer.” Modified, with permission, from Jumars (1993).

(thereby lowering C_o) and (or) *increasing* its size while maintaining the same C_o . The former, in turn, is accomplished by either increasing the affinity (rate of operation) of individual absorptive sites for the substrate (lowering K_m of the Michaelis-Menten formulation) or (and) by increasing the number of absorptive sites on the cell surface (raising V_{max}). For a cell of a given size, however, there is an absolute limit to the increase achievable. This point is made eloquently for phytoplankton in the work of Morel and co-workers on metal uptake (*e.g.* Morel *et al.*, 1991).

In any case, there is no point in seeking or imagining a biochemical means for enhancing the flux further than the value of Eq. 4 with C_o set at zero or beyond the efficiency (specific clearance rate) set by Eq. 2, because, for free-living cells of this size, *it is physically impossible to enhance the flux further*. In cells operating below this diffusional limit, uptake kinetics (V_{max} and K_m) play roles in determining gross (and net) flux into the cell in a manner that is simple conceptually but messy algebraically. It is messy enough that it has been rederived several times, notably by Best (1955) in the literature of cell physiology, Powell (1967) and Koch and Coffman (1970) in the bacterial literature, Pasciak and Gavis (1974) in the aquatic sciences, and Horvath and Engasser (1974) in the engineering literature. (Despite the fact that Koch and Coffman [1970] and Horvath and Engasser [1974] published in the same journal, their papers are aimed at different audiences.) For the limited purposes of our exposition, explicit formulation at this level of complexity is not needed. We especially commend, however, the clear exposition of issues and formulations presented by Koch (1985). While the possibility of joint diffusional and enzyme kinetic limitation is recognized by bacterial physiologists and is sometimes modeled explicitly to get more accurate estimates of true enzymatic V_{max} and K_m (*e.g.* Koch, 1982) in physiological research, the issue of physical diffusional limitation in natural environments has not been widely addressed in the aquatic bacterial literature.

Foraging theory suggests a diversity of adaptations in transporters to nutrient limitation and surplus depending on a number of trade-offs (Diamond and Karasov, 1987): caloric payoff from uptake of energy-yielding nutrients, toxicity of some nutrients at high levels, synthetic and maintenance costs of transporters, and fixed daily requirements. According to the reasoning of Diamond and Karasov (1987), one would expect transporters to increase with nutrient concentration for nontoxic, limiting nutrients that also are energy sources but to decrease after some critical concentration for substances that are essential but become toxic at some levels. Some of this potential diversity of adaptation to nutrient levels is demonstrated among the responses of phytoplankton to trace metals (Morel *et al.*, 1991) and the responses of bacteria to glucose levels (Azam and Hodson, 1981)

A powerful concept of optimal foraging theory that allows refinement of these predictions is the notion of marginal gain in the context of net gain per added transporter. No transporters should be added when the cost of an additional transporter exceeds the increment of gain realized from it. The relationship between areal coverage of the cell with transporters and the fraction of the maximal flux achievable (Eq. 4 with $C_o = 0$), assuming that a transporter occupies a circular area of radius s on the surface of a cell (Fig. 2) and that contact of a nutrient molecule results in

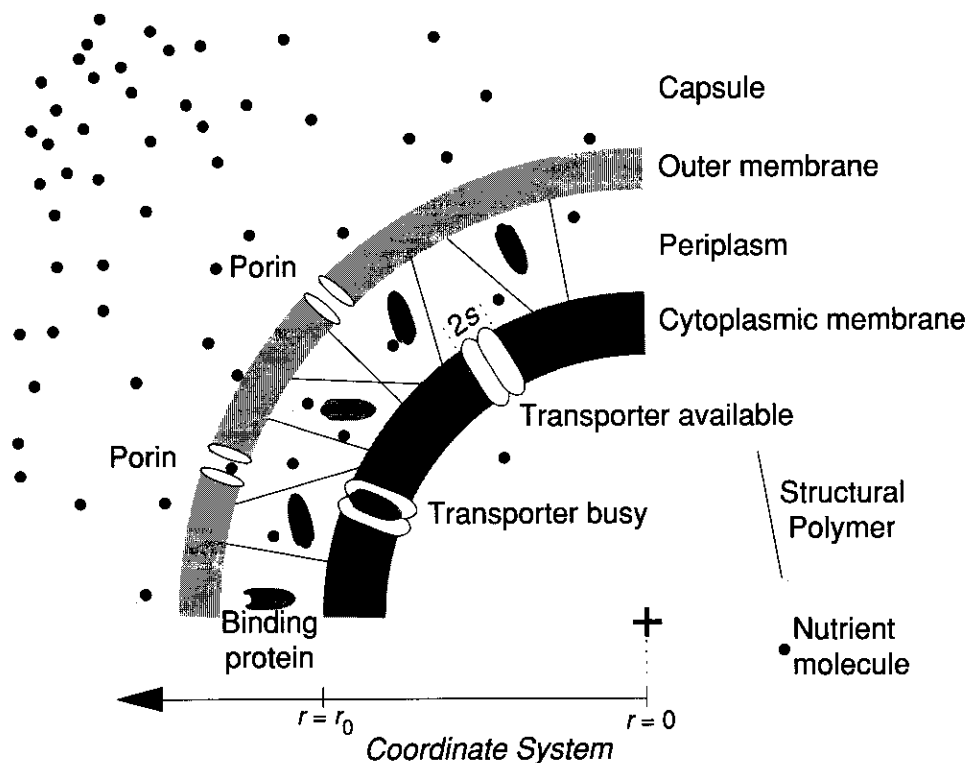


Fig. 2. Typical structure of a Gram-negative bacterial cell placed in the reference geometry of the text. The outer capsule, when present, is thought to be a diffusion-permeable gel. Porins, even at low areal density, provide little impedance to diffusion of small nutrient molecules. The effective radius of a transporter to external (to the cell membrane) encounter by nutrient molecules is given by s . Based on the recent review by Nikaido and Saier (1992).

absorption (the disc being a perfect sink), has been calculated by Berg and Purcell (1977), based on analogy with electrical capacitance:

$$J'_D = J_D \frac{Ns}{Ns + \pi r_0} \quad (5)$$

Here J'_D is the flux achieved with only the indicated coverage of absorptive sites compared to the flux when the entire surface area is absorptive (J_D , Eq. 4) and N is the number of absorptive sites. This flux plateaus at a remarkably small percentage cover of the cell surface (Fig. 3) and reaches one-half of its maximal value (*i.e.* $J'_D/2$) when $N = \pi r_0/s$ and only 0.079% of the cell surface is covered by transporters (assuming that they are spread evenly or randomly about the cell surface). The counterintuitively high efficacy of a small number of transporters comes from two effects. One is the high

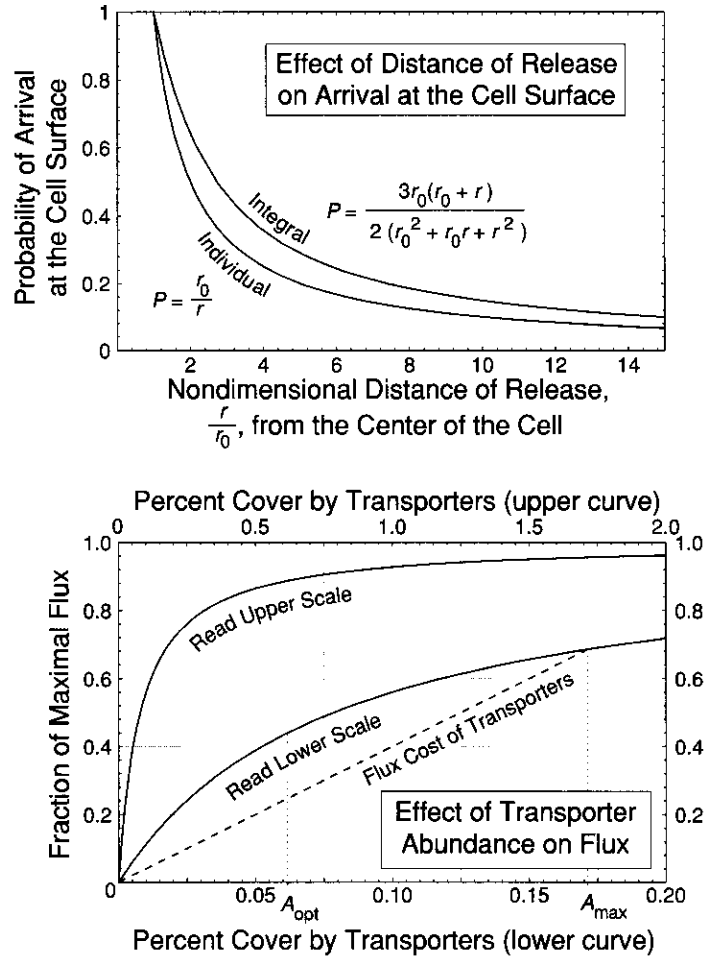


Fig. 3. Further effects of geometry on encounter of nutrients by spherical cells. A molecule released at a set distance $r \geq r_0$ from the cell has the probability labeled “Individual” of diffusing into contact with the cell membrane (Berg and Purcell, 1977). Suppose uniform release over the range of distances from r_0 to r . By integration one then gets the curve labeled “Integral” (Jackson, 1987). The “Individual” curve is relevant to the issue of free release of enzyme, which will yield little return when products are formed more than a few radii from the cell surface, and the “Integral” curve is relevant to substrate production by hydrolytic enzymes immobilized in the periplasm or capsule over a range of distances from the cell. Assuming instantaneous, perfect absorption, surprisingly few transporters are needed to gain nearly the same total flux as would be achieved by having the entire surface be a perfect absorber (Berg and Purcell, 1977). If one assumes a cellular growth rate limited by the rate of acquisition of energy and that each transporter costs the same amount of energy per unit of time to build and maintain it is easy to calculate a total cost (dashed line). Assuming that 40% of the maximal flux achievable is required to synthesize and maintain 0.1% of the surface in absorbers, there is an optimal coverage (A_{opt}) that gives the highest net rate of energy gain and beyond which the marginal gain per transporter drops below the marginal cost per transporter. Above A_{max} , additional transporters would cost more than they could return.

likelihood that a molecule released within a distance of one cell radius or less from the cell surface will strike the cell (Fig. 3). The other is the high likelihood that a molecule will hit the cell surface several times before leaving its vicinity once it has approached within a few molecular step lengths (Berg and Purcell, 1977; Waite and Stewart, 1993). Similar arguments (Berg, 1983; Cussler, 1984; Koch, 1990) show that even with few porins there is little impedance to diffusion through the outer membrane (Fig. 2). The foraging consequence of the efficacy of a few transport sites is that the marginal rate of gain per transporter drops rapidly as the plateau is approached (Fig. 3), making high surface-area coverage by transporters unlikely, even by transporters of the nutrient whose rate of supply chronically limits growth. If the substance being transported no longer is growth-rate limiting or becomes toxic at higher uptake rates, then the marginal rate of gain from adding additional transport sites can drop precipitously.

There are real and apparent complications. Low affinity of a transporter for the substrate (ability of a molecule to bounce off a seemingly ready transporter) or a long time to return a transporter to a ready state (Fig. 2) will increase the number of transporters needed to achieve a given flux over the number predicted from the perfect-absorber model (Eq. 5). Specifically, N in Eq. 5 must be multiplied by $1/P$, where P is the probability that a molecule intercepting an absorber will be caught rather than bounce off. In phytoplankton, for example, some metal-binding systems appear to have slow kinetics, necessitating the multiplication of absorptive sites (Hudson and Morel, 1993). At very high cell coverage by transporters for a specific nutrient, Eq. 5 breaks down (Berg and Purcell, 1977). With respect to pattern of coverage, Maddock and Shapiro (1993) reported that chemosensory sites of *E. coli* are clustered rather than spread evenly over the cell surface. Such clustering would not be expected of uptake sites because it would decrease the flux (Berg and Purcell, 1977) and hence the marginal rate of gain. It is not surprising in sensory rather than absorptive sites, however, because it affords a greater dynamic range for the sensor (saturating at a higher nutrient concentration) than would a comparable number of sites distributed randomly or evenly.

The geometry of diffusion influences nutritional strategies in other ways as well. Gram-negative bacteria have considerable machinery external to the cell membrane (Fig. 2). When small food molecules that can be absorbed directly are lacking, extracellular enzymes can be induced. Their free release in a diffusive planktonic environment is obviously not cost effective. Their immobilization on the cell membrane, in the periplasm, on the outer membrane or in a capsule (Pugsley, 1993), however, is surprisingly effective, however, so long as they are immobilized within a few radii of the cell membrane (Fig. 3). Note, however, how rapidly the value of an immobilized enzyme drops with its distance of deployment. This geometry suggests that those enzymes with the highest costs of production, scarcest substrates and highest values of products will be deployed closest to the cell membrane (Vetter and Deming, in prep.).

Optimal foraging theory immediately allows one to draw conclusions about an optimal cell size. Unless C_0 varies systematically with r_0 , however, gross uptake rate

will vary linearly with cell radius (Eq. 4). Cell catabolism or rate of use of a substrate in growth ($\text{mol cell}^{-1} \text{time}^{-1}$), on the other hand, varies as r_0^a , where all authors agree that $3 > a > 1$. The simple implication of a linear gross gain coupled with a nonlinear gross loss with respect to cell radius is that an optimal cell size exists and increases with increasing substrate concentration (Jumars, 1993). Explicitly, if we assume that Eq. 4 represents gross gain and take gross loss as mr_0^2 , where m is the coefficient for catabolism, optimal cell size can be solved by setting the derivative of the difference equal to zero, yielding a prediction of $r_{\text{opt}} = 2\pi D(C_\infty - C_0)/m$. This same optimization argument is made graphically by Jumars (1993, his Fig. 4.12). Optimal cell size thus varies directly with both the diffusion coefficient and $(C_\infty - C_0)$ and varies inversely with the catabolic coefficient. This simple inference at once explains the common observation of larger cell size under eutrophic conditions. Specialists on rapidly diffusing molecules should be larger in general than specialists on slowly diffusing molecules. Comparable inferences are much more difficult to draw if one focuses on efficiency (Eq. 1) because costs and benefits are not distinguished clearly.

More realistic still in predicting or evaluating optimal size would be the incorporation of other effects on fitness as a function of size, in particular the risk of predation. Bacteria are unusual in the physical difficulty of their capture by predators (Fenchel, 1984). Of all potential mechanisms of encounter, only direct interception and Brownian diffusional deposition can be effective (Shimeta and Jumars, 1991). Per bacterial cell, the rate of encounter by Brownian diffusional deposition drops off with increasing r_0 , while the rate of encounter by direct interception rises. The net result is a size refuge that is apparent whether (Shimeta, 1993) or not (Jumars, 1993, Fig. 14.3) one takes into account the details of bacterivore-specific feeding currents and morphologies. There is no physical mechanism that is efficient at encountering these low-density hydrosols (particles suspended in water) that have r_0 between 0.1 and 1.5 μm . There may be strong selective forces, then, against leaving this general size range even if doing so would yield rapid growth in the absence of predators. Approaches already have been developed (*e.g.* Gilliam, 1989) that could allow one to predict an optimal size under constraints of simultaneous nutrient limitation and predation.

Effects of temperature

Anticipated temperature effects on biota need to be segregated by time scale. We consider first the short-term effects, where short implies a period too short to allow increased numbers of transporters or other changes in biochemical complements of a cell — too short for substantial acclimation or adaptation. For an isolated chemical reaction, including enzymatic ones, the usual effect of a 10°K increase in temperature over the normal aquatic range (273-303°K) is a doubling of reaction rate (Atkins, 1982). Short-term changes in *net* rates resulting from coupled reactions, such as net production rates in autotrophs whose anabolic and catabolic reactions both are affected by temperature change, are not so straightforward to predict, but even here dominance

by a single reaction that conforms to the usual temperature relation has been suggested (*e.g.* Li *et al.*, 1984).

Much less widely appreciated, however, is the fact that the diffusion coefficient (D) [$L^2 T^{-1}$] also changes with temperature, albeit more gradually than does a typical reaction rate. The simplest formulation that reasonably accurately indicates temperature dependence of the diffusion coefficient of a wide variety of solutes is the Stokes-Einstein equation:

$$D = \frac{k_B \tau}{6 \pi \mu R_0} \quad (6)$$

where k_B is Boltzmann's constant, τ is temperature ($^{\circ}K$), μ is dynamic viscosity [$M L^{-1} T^{-1}$] of the liquid solvent, and R_0 is the molecular radius of the solute. The denominator is the resistive force to diffusion, simply drag on a sphere as calculated from Stokes law. The numerator is the corresponding driving force, the chemical potential gradient (Cussler, 1984).

Many empirical and analytic improvements have been made to the Stokes-Einstein equation, but they in general affect the absolute value of D far more than they affect its temperature dependence (*e.g.* Cussler, 1984, his Table 5.2–3). The greatest departures from expectation for both D and the temperature dependence arise when the solute molecule is less than five times larger than a water molecule, for under those circumstances, the continuous nature of the drag force assumed in the Stokes derivation breaks down. Li and Gregory (1974), based on direct tracer measurements suggest that the temperature dependence for molecules diffusing faster than fluoride ions (*i.e.* NH_4^+ , H^+ and OH^- among other biologically important ones) scales approximately inversely with dynamic viscosity — that the direct linear dependence on absolute temperature in the numerator of Eq. 6 disappears. An alternative approach for estimating the diffusion coefficient is to replace the driving force with the electrical potential of the ion in question, yielding the Nernst-Einstein equation (Atkins, 1982). This approach recently has been highly successful in predicting the diffusion coefficients of aqueous species at the high temperatures and pressures of hydrothermal systems (Oelkers and Helgeson, 1988; Oelkers, 1991). We avoid this added complexity because we aim at the temperature dependence of D rather than at calculating D for specific molecules and because we want a parameterization that also will apply to uncharged chemical species. Over the temperature range that we consider, however, again the temperature dependence of the alternative formulations are not very different.

The temperature dependence of D is stronger than one might suspect from casual inspection of Eq. 6. Dynamic viscosity of most liquids is a stronger function of temperature than is the numerator of Eq. 6 and varies inversely with it (Fig. 4), so that the driving force for diffusion increases linearly while the resisting force decreases even faster with temperature. The temperature dependence of μ — and consequently of D — is strongest at low temperatures (Fig. 4). If diffusion rate is limiting over the experimental range, then one can calculate temperature dependence from Eq. 6 and the

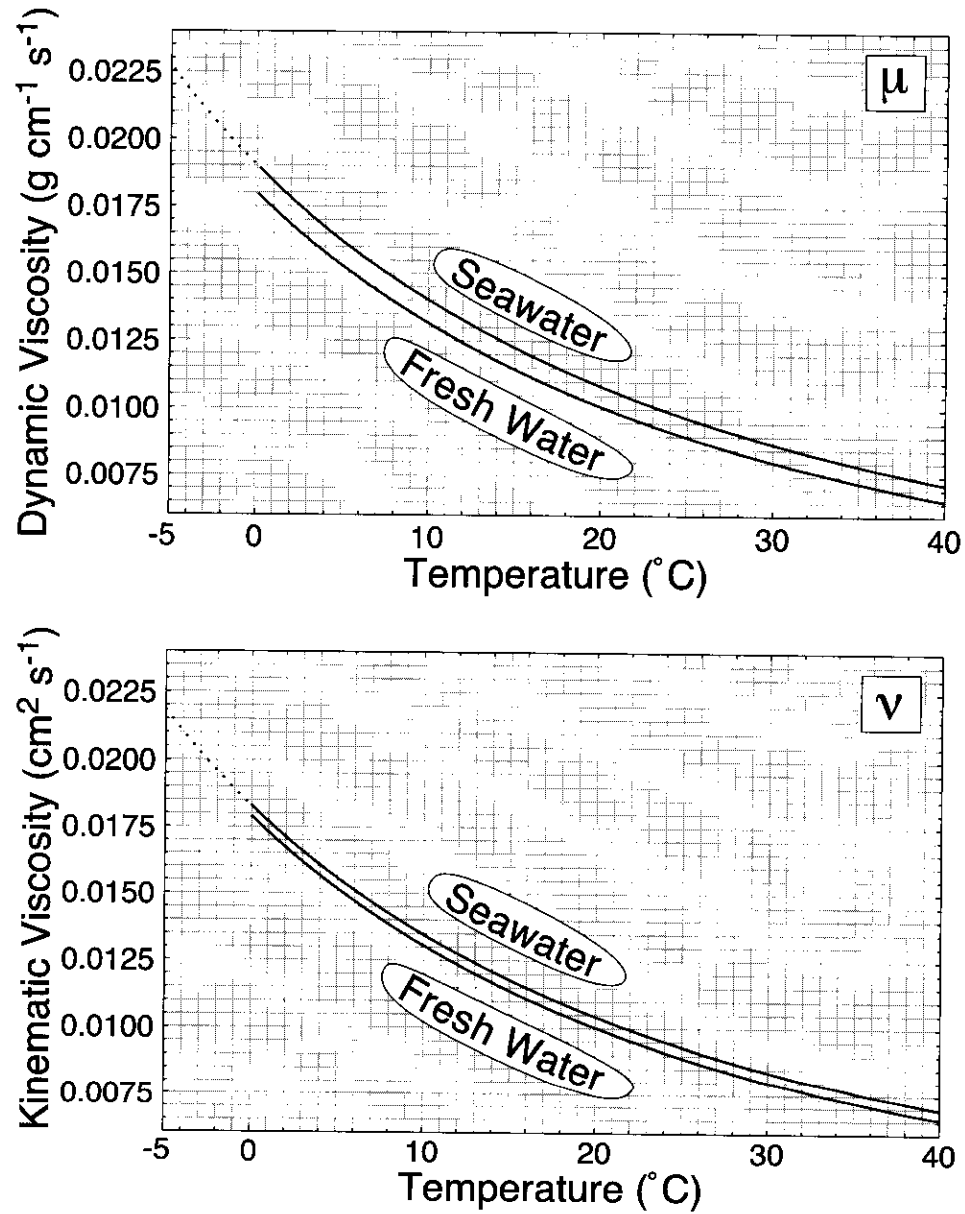


Fig. 4. Dynamic (μ) and kinematic (ν) viscosity versus temperature calculated according to the formulas given in *Appendix*. In each case the upper curve is for seawater (35‰) and the lower curve is for fresh water. No values are given for fresh water below 0°C, and that range for seawater (dashed) is an extrapolation beyond the domain of reliable published data.

relevant (μ_{sw} or μ_{fw} in *Appendix*) viscosity equation. For a seawater temperature change between 0 and 10°C, for example, where numerical subscripts indicate temperature (°C):

$$\frac{D_{10}}{D_0} = \frac{\tau_{10} \mu_{0sw}}{\tau_0 \mu_{10sw}} = \frac{283.15 (0.0188)}{273.15 (0.0138)} = 1.41 \quad (7)$$

For a rapidly diffusing ion (*cf.* Li and Gregory, 1974) the expected dependence decreases only slightly to 1.36, calculated by leaving the absolute temperatures out of Eq. 5. Thus, if diffusion rate limits growth rate over this entire temperature range, one can expect a Q_{10} for growth of about 1.4. For comparison, the Q_{10} calculated similarly between 20 and 30°C is 1.29 for slowly diffusing ions and 1.25 for rapidly diffusing (small) ones. Published Q_{10} values often exceed these levels, but high-latitude bacterial uptake data for some substrates, sample types, regions and times fall within and even below the range of values that could be explained by diffusion alone (*e.g.* Delille *et al.*, 1988; Yager, *in prep.*). Delille *et al.* (1988), in fact reported a Q_{10} of 1.4 for field populations adapted to -1.75 to 0°C — exactly what we would predict if diffusion accounted for the *entire* effect.

Does one expect to see diffusion- or reaction-rate limitation in a field- or laboratory-acclimated culture? Because the gain per transporter drops under diffusional limitation but the cost does not, one expects to see a matching between capacity of active uptake systems and diffusional arrival rates for growth-rate-limiting molecules (Koch, 1971). While this matching of active uptake rates and diffusion is not fully achieved under some incubation conditions (Koch and Wang, 1982), it is approached frequently and closely enough that equations for joint limitation, already cited above, are often useful.

Normal practice in assessing thermal dependence of cellular growth rates is to maintain a culture at a fixed temperature (T_a , for acclimation temperature) or to draw cultures from a field acclimation temperature that is slowly varying compared with a Q_{10} trial. To estimate temperature dependence of growth rate, temperature is changed quickly in subsamples of the culture. At the acclimation temperature, one might expect diffusional fluxes and active uptake rates to be roughly balanced. If temperature is raised, then one should expect to see the onset of diffusional limitation since the uptake reaction has a greater Q_{10} than does diffusion, and the apparent Q_{10} for overall uptake and growth rate upon rapid temperature increase should approach the diffusional determined value of 1.2 to 1.4 (until denaturation sets in). Conversely, if one lowers the temperature, the greater temperature sensitivity of active uptake should produce a Q_{10} for growth that approaches 2 when growth rate is limited by a single reaction having typical temperature dependence. Q_{10} values as high as 8 or more are reported for specific enzymatic reactions (Segel, 1975), however, so the temperature dependence for a specific reaction could be much steeper. Reactions coupled *in series* will proceed at the rate of the slowest one. Therefore the one with the *largest* Q_{10} in the series will become limiting as temperature is lowered, and the one with the *smallest* Q_{10} will become limiting as temperature is raised. Cell growth rate, however, depends on many complex series of reactions proceeding *in parallel*. As temperature is

lowered and each series slows to its most temperature-sensitive component reaction, there will be shifts among series of reactions that are limiting, toward the most temperature-sensitive series. In short, Q_{10} of a complex biochemical reaction-diffusion process like cellular growth must increase as temperature decreases and vice versa. We suggest that these shifts among the reactions that are limiting and between diffusion-rate and reaction-rate limitation underlie the nonlinearity in Arrhenius plots of bacterial growth rates and are a reason (besides simply having more fittable coefficients) that the logarithmic model of Ratkowsky *et al.* (1982, 1983) provides a better fit than do simple Arrhenius plots. This suggestion echoes the conclusion of Bělehrádek (1926) that viscosity has something to do with the problem, though we suggest that diffusion rate (dependent upon viscosity) outside the cell where length scales are greater is more likely to limit growth than is diffusion rate within the cell. A less general explanation would have difficulty treating the range of phenomena, from growing plant cells to rotting fish, that fit the square-root model (McMeekin *et al.*, 1988).

Real Q_{10} estimates require a finite interval. If they are based on isotopic estimates of uptake rates, a small fraction of a doubling time may suffice, with limited possibility for adaptation to the new temperature through, for example, a change in the number of transporters per cell. If the Q_{10} estimate is for population growth rate, then a longer interval is required, with greater opportunity for adaptation.

Temperature acclimation and adaptation

On the longer time scales at which enzyme complements can be modified and cell size can be changed, other responses to temperature are possible. It is entirely feasible to see comparable metabolic rates in two organisms adapted to vastly different temperatures. Such temperature compensation is well known for cold-water versus warm-water species of invertebrates: so long as caloric resources are available, it is feasible for cold-water species to operate at high biochemical rates. It is achieved by altering enzyme concentrations (changing V_{max}) or enzyme affinities (K_m) or by changing the biochemical pathway entirely (Hochachka and Somero, 1984). Bacteria also can be active at very cold temperatures if nutrients are replete (*e.g.* Kottmeier and Sullivan, 1988; Thingstad and Martinussen, 1991; Pomeroy *et al.*, 1991). If transport rate is limiting for a bacterial cell, however, the only avenues open to adaptation in Eq. 4 are cell size (r_o) and the biochemical determinants of C_o . At a lower temperature, the diffusive flux to a cell will be decreased if C_o and r_o remain constant. Again, there is no means for enhancing flux beyond the rate calculated by Eq. 4 for $C_o = 0$ at a given r_o : external transport limitation cannot be overcome by a physiological mechanism short of one that alters r_o or the external environment (D or C_∞). Cells under chronically low rates of supply imposed in a chemostat do approach an active uptake rate that equals diffusional arrival, but natural oligotrophs from aquatic environments do not seem to do so (Koch and Wang, 1982). We explore one way out of this paradox in the subsequent section on time-varying environments.

It also should be apparent from the preceding section that temperature adaptation and nutrient adaptation are difficult to separate for an osmotroph. If temperature increases, decreasing D , nutrient concentration remains the same and the cell reduces nutrient concentration to the same level at r_0 , then higher temperature will produce a higher rate of nutrient supply to the cell. Thus one should expect to see what is observed, *i.e.* an interaction between temperature and nutrient effects at low nutrient concentrations where the cellular transport system is not saturated (Pomeroy *et al.*, 1991). Eq. 4 can be used to predict both the magnitudes of individual effects and the strength of the interaction after including the possibility of uptake kinetic limitation (Pasciak and Gavis, 1974).

In stagnant waters, one would expect photoautotrophs to have a relative advantage over heterotrophic osmotrophs because their energy source, the flux of photons, is not impeded at low temperatures. Thus they would depend on diffusion only for mass acquisition. Bacterivores that feed by Brownian diffusion (Shimeta and Jumars, 1991; Shimeta, 1993) would be affected similarly to osmotrophs, since Eq. 6 applies directly to Brownian motion if R_0 is simply redefined as the radius of the diffusing particle. Bacterivores that are active suspension feeders incur costs of transporting water that are proportional to the dynamic viscosity of the medium, suggesting a slightly lesser dependence on temperature than that seen for diffusive flux (Fig. 4). Whether this temperature dependence is important to the foraging success of bacterivores depends upon the costs of producing fluid motion, which are usually, but not always (Mitchell, 1991) calculated to be small for organisms using flagella or cilia.

Cells in a homogenous, turbulent ocean

One might suppose that diffusive transport limitation could be alleviated by fluid motion. To alter the flux calculated by Eq. 4, however, would require that there be deformation of the diffusional shell described in Fig. 1, enhancing flux by steepening the concentration gradient (dC/dr). Turbulent motions, however, fail to penetrate much below the Kolmogorov scale, L_K , which is calculated as:

$$L_K = \sqrt[4]{\frac{\nu^3}{\epsilon}} \quad (8)$$

where ν is kinematic viscosity [$L^2 T^{-1}$] and ϵ is turbulent dissipation rate [$L^2 T^{-3}$]. Kinematic viscosity, in turn, is defined as μ/ρ , where μ is the dynamic viscosity already defined above and ρ is simply the fluid specific gravity [$M L^{-3}$]. At 0°C in seawater of 35‰ salinity, $\rho = 1.02811 \text{ g cm}^{-3}$ and $\mu = 0.0188193 \text{ g cm}^{-1} \text{ s}^{-1}$, yielding $\nu = 0.0183048 \text{ cm}^2 \text{ s}^{-1}$ (Appendix). Kinematic viscosity differs slightly less than does dynamic viscosity between fresh and salt water because of the offsetting effects of dissolved ions on density and dynamic viscosity (Fig. 4). A reasonable value for ϵ in the upper mixed layer during energetic events is about $10^{-2} \text{ cm}^2 \text{ s}^{-3}$, yielding $L_K = 0.157 \text{ cm}$. If one changes the temperature to 30°C but leaves ϵ the same, L_K is reduced to 0.0878 cm. So many decimal places are given here only to allow readers to compare

their own calculations. Because Eq. 8 is based on a scaling argument, the precise value of L_K must be determined by experiment. In general, a scaling argument will be good only within a factor of about five, so until experiment verifies the prediction, only one significant figure should be claimed for the calculated magnitude of L_K . The issue boils down to how frequently turbulent vortical motions penetrate to smaller scales than the one specified by Eq. 8, an issue potentially not well treated by such a first-moment (mean condition) calculation.

From these calculations, it is plain that temperature, through its effect on kinematic viscosity, has an effect on L_K . For the remainder of the text, however, we will fix kinematic viscosity, ν , at 0.01 for our calculations and the corresponding illustrations. We do so to avoid complex formulas and because the effects on D (through μ) and on ν largely but not completely offset each other in comparisons of advective versus molecular diffusive transport. For simplicity we also leave D set at $1 \times 10^{-5} \text{ cm}^2 \text{ s}^{-1}$ except where noted. We take a range of turbulent dissipations rates (ϵ) from 10^{-4} to $10^{-2} \text{ cm}^2 \text{ s}^{-3}$ as representative of the upper mixed layer in the ocean, though stable density stratification and low energy inputs can yield values of ϵ as low as $10^{-6} \text{ cm}^2 \text{ s}^{-3}$. The full equations are provided should the reader wish to explore larger ranges.

Even if the scaling calculation of L_K overestimates by a factor of 10, however, the extent of the diffusional gradient of Fig. 1 for a bacterium is well below the Kolmogorov scale. Thus, the bacterium experiences only the laminar shear that dissipates turbulence. Whether this shear influences diffusion to the bacterial cell can be determined approximately by the ratio of the characteristic diffusion time through the concentration boundary layer of Fig. 1 (of thickness $9r_0$) to the advection time by the shear over the same distance; one is asking whether the viscous shear could appreciably affect the shape of the concentration profile and thus the flux. Characteristic diffusion times scale as L_c^2/D , where L_c is the characteristic distance (Cussler, 1984), while the characteristic shear-induced velocity, u , over L_c is calculated as (Saffman and Turner, 1956):

$$u = 0.10 \sqrt{\frac{\epsilon}{\nu}} L_c \quad (9)$$

(The leading coefficient of 0.10 is given erroneously as 0.16 by Jumars [1993].) Choosing a typical bacterial cell diameter to be $0.5 \mu\text{m}$, one can see from Fig. 1 that the concentration boundary layer of a bacterium extends only $2.25 \mu\text{m}$ from the cell surface (taking the arbitrary limit to be the point at which $C = 0.9C_\infty$). Thus we choose $L_c = 2.25 \mu\text{m}$, which gives $u = 3.93 \times 10^{-5} \text{ cm s}^{-1}$.

One can then calculate the time for diffusion to carry a molecule over L_c and compare it to the time scale over which the shear-induced relative velocity would carry the molecule the same distance (Mann and Lazier, 1991):

$$\frac{1}{De} = \frac{L_c^2 / D}{L_c / u} = \frac{L_c u}{D} \quad (10)$$

As Jenkinson and Wyatt (1992) pointed out, this nondimensional scaling is properly called an inverse Deborah number (De). Substituting the right side of Eq. 9 for u and setting this De_{cr} at a (cr for critical) value of 1 lets one calculate the approximate size of osmotroph for which shear and diffusion will contribute roughly equally to transport of nutrients over the distance occupied by the concentration boundary layer in still water (Fig. 5). Doing so gives $r_o = 3.5 \times 10^{-4}/\epsilon^{1/4}$.

We go through these rough scaling calculations because they make mechanisms transparent. The problem of shear distortion of concentration boundary layers about phytoplankton has had three other recent analyses by Lazier and Mann (1989), Jenkinson and Wyatt (1992) and Bowen and Stolzenbach (1992). Bowen and Stolzenbach (1992) went beyond a simple scaling argument (De) and applied their results to bacterial chemotaxis (Bowen *et al.*, 1993). They calculated the radius L_d of a central diffusional core that cannot be distorted by turbulence to be:

$$L_d = \sqrt{\frac{D}{E}} \quad (11)$$

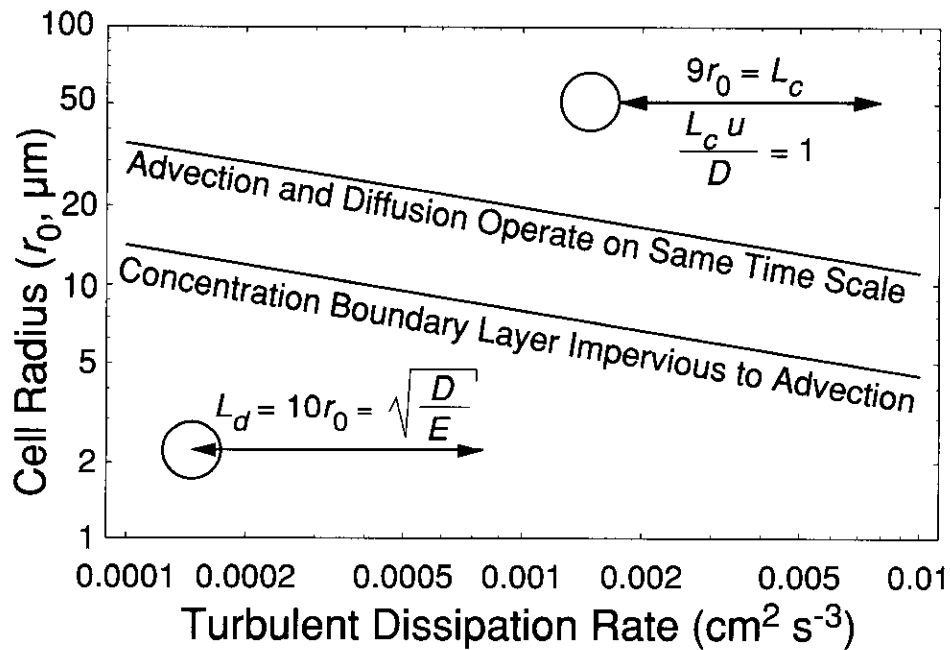


Fig. 5. Cell radii for which the Deborah number (Eq. 10) for time to advect over the thickness of the concentration boundary layer relative to the molecular diffusion time scale over that same distance equals unity and for which the entire concentration boundary layer of Fig. 1 is impervious to advective distortion (Eq. 11). Many if not most phytoplankton cells fall in the range where advection due to shear from turbulent dissipation can alter diffusion geometries and rates.

where E is the shear rate (s^{-1}), in turn calculated as

$$E = 0.5 \sqrt{\frac{\varepsilon}{\nu}} \quad (12)$$

We caution the reader that the leading coefficient of 0.5 is not used universally. Many authors regard the relation between E and ε as a scaling argument, without a leading coefficient (or with an implied coefficient of order unity). Rather than convert all authors' results to the convention of Eq. 12 used by Bowen *et al.* (1993), we instead point out when and where inconsistencies might cause confusion. We use their convention in converting between ε and E in all our calculations. Setting L_D to encompass the concentration boundary layer about the cell (Fig. 5) gives freedom from distortion of this concentration boundary layer by fluid motion when $r_0 \leq 1.4 \times 10^{-4}/\varepsilon^{1/4}$. It is clear from these two bounds (Eq. 10 & 11) that the concentration boundary layers of cells of radius $> 10 \mu\text{m}$ are subject to some distortion. How important that distortion is depends upon the question being asked. Flux to the cell depends most critically on the gradient near the cell surface, and so will not be terribly sensitive to modest distortion at the periphery of the concentration boundary layer. The geometry of an enriched zone of nutrients about a phytoplankton cell from the standpoint of a resource for bacteria (*e.g.* Azam and Ammerman, 1984), however, may be much more sensitive, since the bulk of the volume of this enriched zone ($9r_0$ thick about the phytoplankton in our present definition of the concentration boundary layer) is more than a few radii from the cell.

If one wants a quantitative rather than a qualitative answer regarding the importance of fluid motion to osmotrophs, even the concept of an impregnable core is not enough. The reason can be seen by turning back to Fig. 1. Approach to C_∞ is asymptotic in the absence of fluid motion. In the presence of fluid motion, that motion brings C_∞ closer to the cell, and the whole gradient must readjust (*cf.* Batchelor, 1979, his Fig. 1), despite the fact that advection does not penetrate that gradient; even though a diffusional core may be safe on average from erosion by shear, the concentrations within it will have been changed by reduction or elimination of the gradients outside this core. To anticipate the quantitative results in the light of our Fig. 1, flux begins to increase dramatically, however, only when advection penetrates to distances corresponding with the highest gradients of Fig. 1.

For the problem of nutrient acquisition by a cell suspended in a turbulent medium, one wishes to know the role of shear from turbulent dissipation in mass transfer across the solid-liquid boundary of the cell surface. A relevant nondimensional number is called the Sherwood number, Sh . Sh is defined as the ratio of total mass transfer across a boundary to mass transfer in the absence of fluid motion. With this definition (and we caution that other definitions are sometimes used), Sh must asymptote at a value of unity as the intensity of fluid motion decreases. Flux across the boundary (surface area) toward a sphere in shear flow is defined (Clift *et al.*, 1978) as:

$$J = -4\pi r_0^2 k (C_\infty - C_0) \quad (13)$$

where k is a mass transfer coefficient [$L T^{-1}$]. Substituting Eq. 4 then yields

$$Sh = \frac{J}{J_D} = \frac{kr_0}{D} \quad (14)$$

As pointed out by Logan and Dettmer (1990), several Sh correlations with fluid dynamic variables have been proposed for mass transfer to and from spheres in a moving fluid, and most give poor fit to data (their Fig. 4). Many of these empirical equations stem from the engineering literature of heat transfer and go through the intermediate step of calculating a Péclet number,

$$Pe = \frac{u r_0}{D} = \frac{E r_0^2}{D} \quad (15)$$

and then finding a correlation between some function of Pe and Sh . Pe is inherently easier to estimate or measure than Sh because it is a property of the fluid, while Sh is a flux across a solid-liquid boundary. Here the velocity u does not in general correspond with our choice of u for Eq. 9, and most workers neglect an explicit numerical coefficient for the conversion between ϵ and E (Eq. 10). While the heat transfer literature also uses Pe it replaces Sh with a Nusselt number (Nu), the analogous nondimensional formulation for heat transfer. We caution that some authors quote values of Nu when referring to mass transfer rather than heat transfer. Intuitively, Pe is the ratio in transport rates provided by advection versus by diffusion on the fluid scale of interest. Hence it goes to zero when fluid is completely at rest. An extremely large range of Pe is of interest for the problem of marine osmotrophy in the upper mixed layer. Taking even the narrow bounds that we have chosen for turbulent dissipation rates and a range of osmotroph sizes from 0.25 μm to 0.5 mm in radius, gives a range of interest in Pe from 10^{-6} to 10^2 .

As Logan and Dettmer (1990) also pointed out, part of the poor fit to proposed correlations is due to the combining of data from at least three different flow regimes: spheres in steady, uniform flow (held still in a uniformly flowing liquid or settling at constant velocity through a still fluid); spheres suspended on a filter through which fluid is drawn at a constant pipe velocity (though fluid must accelerate through the smaller pore spaces of the filter) and spheres suspended in a linear shear field such as neutrally buoyant cells smaller than the Kolmogorov scale would experience. Because the flow patterns differ, a different definition of u from Eq. 15 should be employed for each of these flow geometries. Cells on a filter are most analogous to cells attached to surficial sediments or to settling aggregates through both of which pore water can flow (*e.g.* Huettel and Gust, 1992). Another part of the poor fit is due to empirical correlations based on small sample sizes over limited Sh and Pe ranges. Logan and Dettmer (1990) again gave good access to this literature, but there is no consensus resolution.

Lazier and Mann (1989) clearly distinguished the case of settling from suspended cells and provided predictions of the effect of linear shear on mass transfer rates to

osmotrophs suspended in natural turbulence. They provided no explicit equations for Sh , but presented their results graphically. Lazier and Mann (1989) used the empirical results of Purcell (1978) from a heat-transfer experiment to produce their graphs. The case of settling cells certainly may be of interest. We do not treat it further, however, except to note (Batchelor, 1980; Bowen *et al.*, 1993) that the effect of shear will dominate the effect of sinking or swimming on mass transfer so long as the translational velocity is $< 5r_0E$. In the case of modest settling velocities through turbulent waters, then, the treatment we pursue applies.

Again in the spirit of gaining and giving access to relevant equations, we revisit Sh correlation and estimation. We restrict ourselves entirely to the issue of neutrally buoyant or slowly settling cells in homogeneous, steady turbulence. We transform extant equations, where needed, to conform to our definition of Sh and our use of the sphere's radius as the relevant length scale. Batchelor (1979, his Fig. 3) suggested that Purcell's (1978) experimental data, through wall effects, underestimated the exchange rate for particles suspended in an unbounded flow field, though his own later theoretical derivation (Batchelor, 1980) does not support this suggestion for $Pe > 1$. Batchelor (1980) derived an explicit relation between Sh and the turbulent dissipation rate, ϵ :

$$Sh = 0.55 \left(\frac{r_0^2 \sqrt{\epsilon}}{D \sqrt{\nu}} \right)^{\frac{1}{3}} = 0.55 Pe^{\frac{1}{3}} \quad (16)$$

(To be consistent with our definition of Pe in Eq. 15, E of Eq. 12 must equal $(\epsilon/\nu)^{1/2}$). This derivation is based on first principles, an assumption of $Pe \gg 1$ and but one fitted coefficient that can have only a minor effect on the leading term of 0.55. Batchelor (1980) further compared this relationship to extensive chemical engineering experiments and found very good fit to observed mass-transfer rates in the chemical engineering literature for $Pe \geq 50$ (corresponding with $Sh \geq 2$) and turbulent particle Reynolds numbers (Re) in the range $10^{-2} \leq Re \leq 10^2$, where

$$Re = \frac{r_0^2 \sqrt{\epsilon}}{\nu^{1.5}} \quad (17)$$

For a reasonably high value of the turbulent dissipation rate ($0.01 \text{ cm}^2 \text{ s}^{-3}$), Eq. 16 therefore should apply to particles as large as 1 cm. Osmotrophs in the water column fall well below this upper limit. For these reasons we believe Eq. 16 is well suited to aquatic settings when $Pe \geq 50$. If one is concerned only with situations where advection might at least double transport, there is little point in going below this Pe , and one can simply solve for the cell radius or turbulent dissipation rate needed to achieve this doubling ($Sh = 2$).

A much earlier theoretical derivation (Clift *et al.*, 1978) is frequently given for $Pe \rightarrow \infty$, *i.e.*

$$Sh = 1 + (1 + Pe)^{\frac{1}{3}} \quad (18)$$

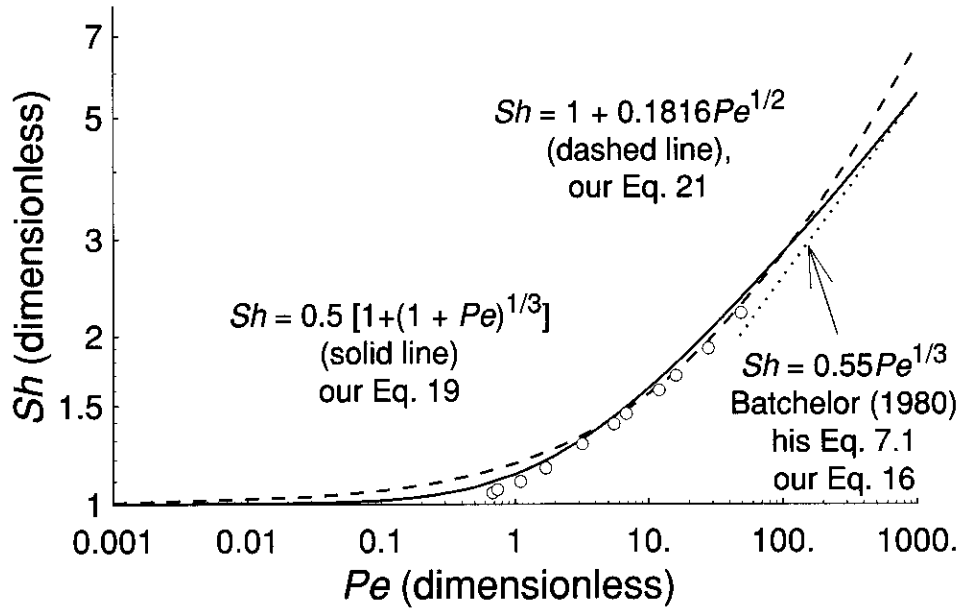


Fig. 6. Sherwood number (Sh) as a function of Péclet number (Pe) over the upper range of interest for marine osmotrophs. Eq. 19 was derived for $Pe \gg 1$, though we extrapolate it to $Pe = 0$. Eq. 21 was derived for $Pe \ll 1$, though we extrapolate it to $Pe = 10^3$. Sh indicates how many times more flux can occur across the surface of a spherical cell in the presence of fluid motion than in its absence, while Pe scales advective mass transport to molecular diffusional transport in the fluid. The 11 open circles are the data of Purcell (1978). Much of the region of interest for marine osmotrophy falls in the poorly understood region near $Pe = 1$, where additional observations and theory are sorely needed. Were it not for the fact that Purcell's (1978) data near $Pe = 1$ fit the high- Pe formulation better and his data in the region $10 < Pe < 100$ fit the low- Pe formulation better, it would be logical to use the crossing point at $Pe = 4.75$ to switch between high- Pe and low- Pe forms.

Note that this form does not asymptote at 1, as it must, when $Pe \rightarrow 0$. Conversely, the two leading digits have very little effect when Pe gets very large. To conform with our conventions, we adopt the form

$$Sh = \frac{1}{2} \left[1 + (1 + Pe)^{\frac{1}{3}} \right] \quad (19)$$

There are *no* fitted coefficients in this formula, yet it follows Purcell's (1978) data extremely well, explaining 98.8% of the variance (Fig. 6). As further, more empirical, justification of our transformation, we fitted Purcell's (1978) data to the form of Eq. 19, but allowed the leading coefficient to vary rather than be fixed at 1/2. This best fit occurs for a value of 0.477 (99.6% of variance explained), surprisingly close to the value of Eq. 19, though the 95% confidence limits (0.472–0.482) do not embrace that value of 1/2.

Theoretical derivations of Sh for low Pe ($\ll 1$) have been available for some time (Frankel and Acrivos, 1968, p. 1916):

$$Sh = 2 + \frac{0.9104}{\sqrt{2\pi}} \sqrt{Pe} + \dots \quad (20)$$

where higher-order terms are omitted (also omitted in Frankel and Acrivos [1968]). Transforming, as before (*i.e.* simply multiplying the right side of Eq. 10 by 1/2), to yield consistency with our conventions yields

$$Sh = 1 + 0.1816 \sqrt{Pe} \quad (21)$$

Again there are *no* fitted coefficients in this formula, yet it follows Purcell's (1978) data extremely well, explaining 99.4% of the variance (Fig. 6). As an empirical, justification of our transformation, we fitted Purcell's (1978) data to the form of Eq. 21, but allowed the coefficient to vary rather than be fixed at 0.1816. This best fit occurs for a value of 0.169 (99.6% of variance explained), and its 95% confidence limits (0.158–0.179) come very close to embracing the theoretical value. We point out, however, that we are unaware of any systematic experimental tests of the Sh - Pe correlation for $Pe \ll 1$.

After the transformations used for Eq. 19 and 21, there appears to be no need for interpolating formulas in the otherwise awkward transition region (*e.g.* Logan and Hunt, 1988) between high- and low- Pe formulas. There is remarkably little difference in the quantitative predictions of the low- and high- Pe forms over the full range of interest in aquatic osmotrophy (Fig. 6). Expressing increased flux due to fluid motion as a percentage amplifies the small absolute difference at low Pe (Fig. 7).

Combining Eq. 21 and Eq. 14, one can estimate the total flux of nutrients to a cell in a turbulent environment:

$$J = - \left(4 \pi r_0 D (C_\infty - C_0) + 1.1614 r_0^2 (C_\infty - C_0) D^{\frac{1}{2}} \epsilon^{\frac{1}{4}} \nu^{-\frac{1}{4}} \right) \quad (22)$$

We write the equation in expanded form so that the first term represents purely diffusional transport in stagnant water (Eq. 4), while the second term adds the contribution of viscous shear from turbulent dissipation. If we change convention to let $E = (\epsilon/\nu)^{1/2}$ then the leading coefficient on the second term changes to 2.282. Note that as the second term becomes larger than the first, dependence on r_0 changes from first order to second order, dependence on ambient concentration remains first order, dependence on the diffusion coefficient drops to a power of 1/2, and ϵ and ν enter at even less influential powers. Combining Eq. 14 and 19, in turn, yields

$$J = - \left(4 \pi r_0 D (C_\infty - C_0) + \pi r_0^5 (C_\infty - C_0) D^{\frac{2}{3}} \epsilon^{\frac{1}{6}} \nu^{-\frac{1}{6}} \right) \quad (23)$$

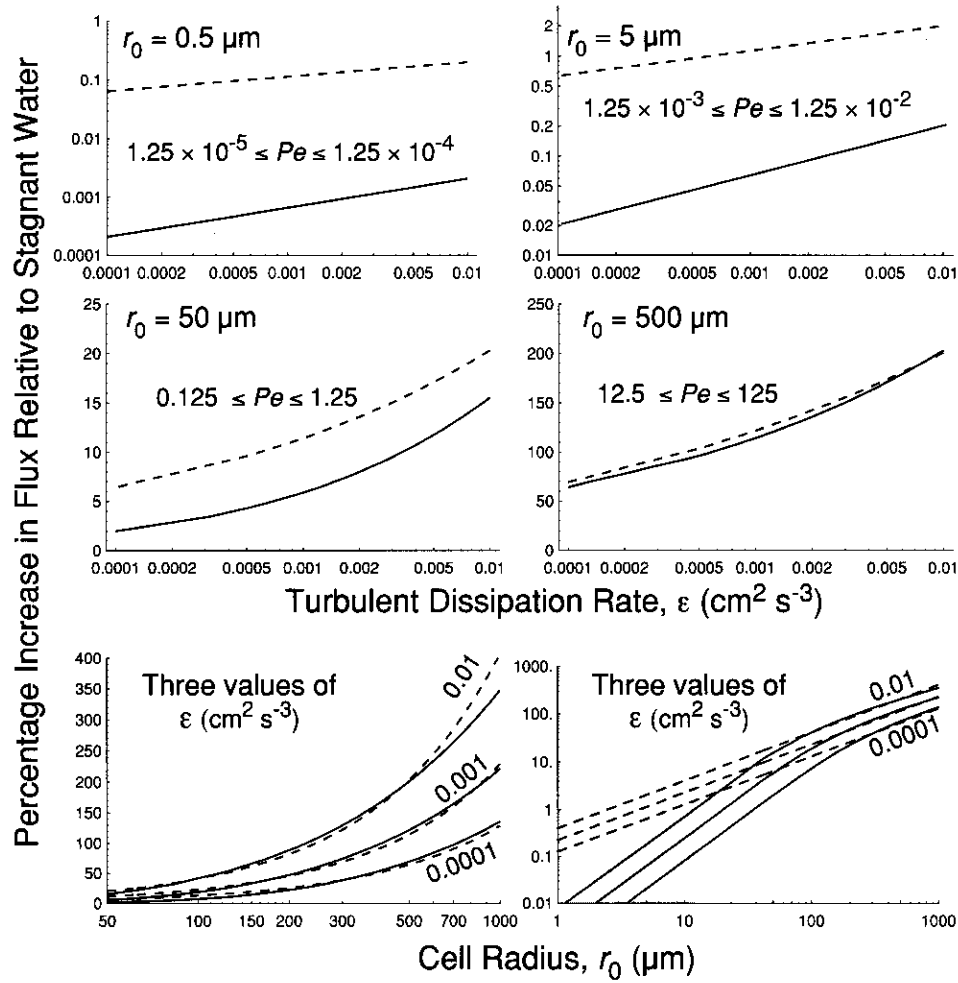


Fig. 7. Effects of both cell radius and shear from turbulent dissipation on transport rate to the cell surface. The solid lines correspond with Eq. 19, derived for $Pe \gg 1$, while the dashed lines correspond with Eq. 21, derived for $Pe \ll 1$. Shading in the lower right panel bounds the region where the effect of fluid motion is negligible ($\leq 5\%$ enhancement over stagnant water *cf.* Eq. 4).

If we change convention to let $E = (\epsilon/\nu)^{1/2}$ then the leading coefficient on the second term changes to 2π . Fig. 7 uses Eq. 22 and 23 as written. While dependence on r_0 , ϵ and ν declines in importance relative to Eq. 22, r_0 retains its dominant effect (Fig. 7) and D increases slightly in importance. While effects of temperature on D and ν are roughly equal in magnitude and opposing in direction, ν exerts a smaller effect in the second term of both equations through its smaller exponent: for a fixed value of ϵ , J is slightly larger at higher temperatures.

There has been some experimental evaluation of the effect of fluid motion on uptake by osmotrophs. Logan and Kirchman (1991) have verified the lack of effect on unattached bacteria for any reasonable field values of ϵ when D is of order 10^{-5} . Their parallel experiments forcing flow past bacteria on a filter nicely confirm that fluid motion can have an effect; free-living planktonic bacteria, however, follow the flow, and so there is no means to raise their mass acquisition rates very high above the level predicted for stagnant water (Fig. 7). Confer and Logan (1991), in turn, showed that even bacteria can be affected by unnaturally high shear levels if macromolecules with low diffusion rates are considered. They used dextran and bovine serum albumin substrates that had D of order $5 \times 10^{-7} \text{ cm}^2 \text{ s}^{-1}$. The shear rates ($E = 200 \text{ s}^{-1}$) used were 400 times larger than the value for active mixed-layer turbulence (0.5 s^{-1}), and barely within the bounds seen near the beds of steep gravel rivers (A. Nowell, pers. comm.). Further, there was no direct measurement of shear. Assuming a cell radius of order $0.7 \mu\text{m}$ (cf. Logan and Dettmer, 1990) yields $Pe \approx 2$ giving (Eq. 20) $Sh \approx 1.2$, a 20% increase over the unstirred state. Confer and Logan (1991) observed growth enhancement due to stirring to be roughly 900% ($Sh \approx 9$). As they pointed out and learned by monitoring protein fragments from BSA digestion, under the high cell densities (10^8 ml^{-1}) and high stirring rates used, some substrate digestion goes on externally to the cell, with products lost from one individual presumably being gained by others: More than simple diffusion of one substrate was going on. In nature, with $E = 0.5$, $D = 5 \times 10^{-7}$ yields $Pe = 0.005$ and (Eq. 21) $Sh = 1.01$, a barely perceptible increase. For leucine, which is absorbed without external hydrolysis, we calculate (Eq. 21) an expected increase in uptake rate of roughly 6% under $E = 200$, whereas 15% was observed. The Sh correlation used by Confer and Logan (1991) fits the leucine data better, and comes from an interpolating function devised by Logan and Hunt (1988) for the Pe region near unity. While tantalizing, the results are too sparse to tell whether our predictive equations (Eq. 19 and 21) are more or less accurate than equations currently in use. Again, however, the overall conclusion is that there should be little effect of natural oceanic turbulence levels on uptake by free-living bacteria in a uniform medium.

For larger organisms, as noted by Lazier and Mann (1989), turbulence clearly can steepen diffusional gradients even for rapidly diffusing solutes and thus can enhance diffusive flux well beyond the level calculated via Eq. 4 (Fig. 7). In this case, rate of advective-diffusive gain rises faster than linearly with cell size, and optimal size can increase radically in a turbulent environment. We suggest that this benefit of large size is one reason that maximal growth rates of large diatoms are not as strongly reduced for large cell sizes as one might otherwise expect (Banse, 1982; Sommer, 1989). It also is a likely contributor to the observation by Pomeroy and Deibel (1986) that phytoplankton outgrow bacteria at low temperature in the field. Although laboratory culture conditions generally are ill characterized with respect to dissipation or shear rates, cultures normally are agitated. Experiments are in order to determine whether natural field shear rates do in fact enhance nutrient acquisition for large phytoplankton. There is some evidence of diffusional limitation in some diatoms in the absence of stirring (Johnston and Raven, 1992; Riebesell *et al.*, 1993). Conversely,

Pasciak and Gavis (1975) provided an elegant demonstration that shear can increase nitrate uptake rate in a diatom of roughly 50 μm radius. Not accounting for shape effects, we would predict (Fig. 7, $r_o = 50 \mu\text{m}$, $\varepsilon = 0.01$) about a 15-20% increase in flux due to shearing at 0.5 s^{-1} , and Pasciak and Gavis (1975, their Fig. 5) found about a 2% increase in net uptake. The offset may be due in part to inaccuracy of Eq. 19 and 21 and in part to greater saturation of the uptake system with increasing shear. Canelli and Fuhs (1976) also demonstrated increased uptake with increased fluid motion, but they held cells on filters through which water passed, making quantitative assessment of our predictions difficult. Whether our proposed equations are accurate or not, it is plain from Fig. 7 that a steep transition in importance of shear will occur over the natural size range of marine phytoplankton. One would expect that large filaments and chains in particular could benefit from unsteady linear shear and from spanning substantial fractions of the smallest vortices (Karp-Boss, in prep.).

Planktonic bacterivores that feed via direct interception will experience an encounter rate that is proportional to $(\varepsilon/\nu)^{1/2}$ (Shimeta, 1993, his Eq. 4), while planktonic bacterivores using Brownian diffusion will experience an encounter rate proportional to $D^{2/3} (\varepsilon/\nu)^{1/6}$, where D is the Brownian diffusion coefficient for bacteria (Shimeta, 1993, his Eq. 5). Shear from turbulent dissipation benefits bacterivores. Note that in either case, for a given turbulent dissipation rate, one expects encounter rate to increase with temperature. The fact that bacterivores are large enough to experience greater shear from turbulent dissipation than does a bacterium can in theory give the bacterivore relative advantage in a turbulent ocean.

Part of the reason for agitation in laboratory cultures is that both batch cultures and chemostat cultures attempt chemical homogeneity. In the jargon of chemical reactor theory (Levenspiel, 1972) in a batch reactor (= batch culture), $\partial C/\partial x = 0$ outside the concentration boundary layer of a suspended cell, where x is any spatial coordinate, and in a continuously stirred tank reactor (= chemostat) both $\partial C/\partial x$ and $\partial C/\partial t = 0$. Less obviously, for large cells this agitation can also prevent diffusional limitation, while for small bacteria it cannot.

Cells in a heterogeneous, turbulent ocean

It is now well appreciated, however, that sources of bacterial and phytoplankton nutrition in nature are not uniformly distributed. They arise from a microscopically and macroscopically time-varying patchwork of continuous and discrete sources (Pomeroy, 1974; Goldman, 1984; Jackson, 1980; Azam and Ammerman, 1984; Jumars *et al.*, 1989; Bowen *et al.*, 1993). Whether bacteria swim or not, shear from turbulent dissipation moves bacteria into and out of regions of high nutrient concentration and thereby causes nutrient sources to appear unsteady to them. An animal excretion event is obviously unsteady (Jackson, 1980; Jumars *et al.*, 1989). The concentration boundary layers of "leaking" phytoplankton occupy relatively little space, and so bacteria distributed at random are unlikely to be in those nutrient-rich shells at any one time (Azam and Ammerman, 1984; Jumars, 1993). This calculation has led to an

interesting series of papers by various authors on the utility of chemotaxis (Bowen *et al.*, 1993, and references therein). The conclusion is that individual bacteria are unable, except during periods of extreme water-column stability, to hover in the vicinity of a nutrient-excreting phytoplankton cell. The benefits are statistical and arise from the greater time spent in diffusional boundary layers of phytoplankton cells during the biased random walk of chemotaxis in turbulent shear. This conclusion and the consequent lack of plausible mechanism for group selection (Table I) together vitiate the suggestion (Azam and Smith, 1991) that unattached bacterial strains can develop a mutualism with phytoplankton strains. The suggestion further lacks the prerequisite of initial gain to both parties for mutualism to evolve (Keeler, 1985) and is untenable in the absence of either physical or evolutionary mechanism. The suggestion would be far more likely for associations in aggregates and benthic environments (Table I). Because bacterial chemotaxis does provide some net gain in the plankton, especially during episodes of high water-column stability (Bowen *et al.*, 1993), it can be explained in terms of ordinary self interest and individual fitness.

Debate about the role of chemotaxis has been so stimulating that it has drawn attention away from the fact that water in motion will bring non-motile, free-living bacteria in contact with patches of high nutrients. Jumars (1993), based on simple coagulation theory, approximated the mean frequency of such encounters per bacterial cell to be:

$$\lambda \approx 0.16 \sqrt{\frac{\epsilon}{\nu}} (d_s + d_b)^3 N_s \quad (24)$$

where d_s is diameter of the concentration boundary layer or "diffusional shell" of the phytoplankton and d_b twice the radius of the bacterium, respectively, and N_s is the number of shells (leaking phytoplankton cells per unit of volume). For the case considered by Azam and Ammerman (1984, *i.e.* 10^3 leaking phytoplankton cells of 20- μm diameter cm^{-3} of seawater) and $\epsilon = 0.01 \text{ cm}^2 \text{ s}^{-3}$, a bacterium should experience an encounter on the order of every 13 min if the concentration boundary layer is not substantially eroded. If one instead conservatively reduces d_s to $2L_d$ of Eq. 11 = 89 μm to account for turbulent erosion of the concentration boundary layer, however, encounter frequency drops to 0.43 h^{-1} (Fig. 8). None of these calculations includes encounter with digestive by-products, another source of unsteady supply (Lehman and Scavia, 1982; Jumars *et al.*, 1989). Jumars (1993) also argued that encounter frequencies of bacteria with phytoplankton concentration boundary layers should be roughly exponentially distributed. Specifically, he suggested that the probability of a given interval t between encounters can be estimated as:

$$f(t) = \lambda e^{-\lambda t} \quad (25)$$

If so, then over 63% of bacterial cells will encounter shells within a period of λ^{-1} (Jumars, 1993, his Fig. 10.3). How should bacteria respond to such encounters and what is the evidence that they do?

We start our analysis with well-known phenomena and from the protoplasm outward. Bacteria are well known for their capabilities of enzyme induction, that are well understood qualitatively in terms of optimal foraging theory. The cell should not bear the cost of making an enzyme constitutively if net rate of gain is improved by making it only when it is needed. It is important in order to treat this question to separate it from well-established but relatively long-term adaptation to nutrient fluctuations. In his now classic analysis of the feast-and-famine existence of *Escherichia coli* (Koch, 1971) notes that this species and others carry more RNA than would be expected during starvation in apparent readiness for the next boom cycle; his analysis shows that net long-term growth rate can be enhanced in this way. Likewise, cells carry internal storage products that are formed at the end of boom cycles in sufficient quantity to last until the next boom cycle (Parnas and Cohen, 1976). These analyses, however, are based on boom-and-bust cycles of order 3 d^{-1} , whereas the

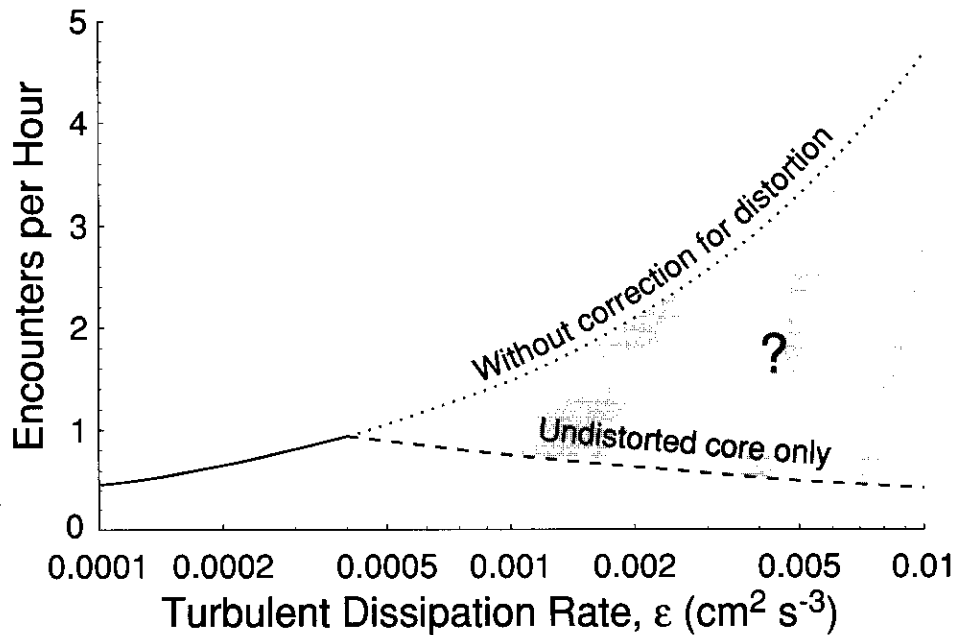


Fig. 8. Predicted encounter frequency of individual bacteria with the concentration boundary layer of phytoplankton cells $10 \mu\text{m}$ in radius at $10^3 \text{ cells ml}^{-1}$ due to laminar shear from dissipation of turbulence. The uncorrected curve assumes that the concentration boundary layer is a sphere of $200 \mu\text{m}$ diameter. The curve labelled "Undistorted core only" uses Eq. 11 as a lower bound for the radius of the concentration boundary layer. The true relation probably falls somewhere in the shaded zone but might even fall above it. Accurate theory would incorporate the effect of shape distortion of the concentration boundary layer into tubes and discs (Bowen and Stolzenbach, 1992). In any case, non-motile planktonic bacteria benefit from nutrient-rich encounters 10 or more times per day and perhaps 100 times per day in energetic regimes.

encounter cycles calculated above are of order 10 d^{-1} or more. The former are near to peak doubling times of cells and hence are compatible with major changes in cellular machinery, but the latter are much less so. This high frequency drives our focus on the transport machinery of cells over very short time scales. Morel (1987) recently has reviewed transport kinetics, but again his focus is on longer intervals over which steady-state solutions of his presented equations can apply. We consider primarily the short term wherein neither the number of transporters nor the cell quotient for a particular nutrient changes significantly. We deal here with steady-state solutions only to the extent necessary to place transients in their context. The transients upon which we focus are not due to structural changes in cellular apparatus but rather to the response of a fixed physiological apparatus to an unsteady stimulus. Is the apparatus structured to take advantage of or at least to modulate excursions in nutrient concentration?

To begin addressing this question, first strip away the periplasm and outer membrane (Fig. 2) and consider a number n of transporters. For the sake of argument and simplicity, take the time from arrival at the outside of the transporter to delivery of the nutrient molecule into the protoplasm — with the transporter only then ready to accept a new molecule — as a constant, q [T]. The capacity of this transporter system (V_{max}) then must saturate in either steady or unsteady mode at a transport rate [N T^{-1}] of n/q . Assume for the moment that the only path of arrival is directly from the outside medium and that a molecule that arrives while the transporter is busy simply bounces away. Again for simplicity assume Poisson arrival rate of molecules at these “correct” spots. The average processing rate for the cell at steady state then must include a correction, λ , the mean time to arrival at a just-readied transporter:

$$V = \frac{n}{q + \lambda} \quad (26)$$

Dividing both numerator and denominator by q gives a more familiar form:

$$V = \frac{V_{max}}{1 + \frac{\lambda}{q}} \quad (27)$$

Noting that ambient concentration C of the nutrient should be inversely proportional to λ , that is, $\lambda = k/C$, one can then reproduce the Michaelis-Menten formulation:

$$V = \frac{V_{max} C}{C + \frac{k}{q}} \quad (28)$$

Paradoxically, if the cell has been starved for a period in excess of q , then all transporters are ready, and n molecules can be grabbed instantly, while if the cell has

been very busy, very few transporters are available to newly arriving molecules. This transient behavior has some capability to explain rapid initial uptake, especially if both n and q are large. Cooperativity, the ability of a single transporter to handle multiple substrate molecules at one time with lower q per molecule, is one way to take greater advantage of transients.

In the limit, take short, infrequent pulses of nutrients, so short that a transporter cannot act on two molecules in succession and so infrequent that all transporters are ready when a pulse occurs. Assuming constant number of transporters per unit of area, one then finds that net flux of nutrients into the cell should be proportional to r_0^2 not r_0 of Eq. 4. That is, infrequent pulses of nutrients should favor larger cells, as has been demonstrated experimentally for phytoplankton (Suttle *et al.*, 1987, 1988).

As the smallest of all free-living organisms, bacteria would appear to have a serious difficulties under these conditions. Going one layer out from the cell membrane, however, periplasm constitutes 20-40% of total "cell" volume and contains binding proteins for nutrients (Neidhardt *et al.*, 1990). At steady state, such binding maintains a concentration gradient that keeps diffusion going in the right direction. We suggest that in unsteady state, it provides a reservoir of nutrients to be filled upon encounter with rich pulses and processed more slowly and steadily by the active transport system of the cytoplasmic membrane. Even if they desorb and simply diffuse, molecules held so close to the cytoplasmic membrane are very likely to strike it by diffusion (Fig. 3). Bacterial capsules (Cowen, 1992) also are likely to be useful for such temporary storage and for the immobilization of enzymes, whose products are still likely (Fig. 3) to hit the cell membrane.

The methods of queueing theory (Allen, 1990) are suited elegantly to analysis of this problem. What we are suggesting specifically is that the periplasm and perhaps the capsule constitutes a "waiting room" that keeps "customers" from leaving when all the transporters are busy. In the shorthand of queueing theory, we suggest that the extra-cytoplasmic portion of the cell can be modeled as a $GI/U/n/K/\infty/RSS$ queueing system, where GI indicates a general independent interarrival time to the transporter (which may fit an exponential or an Erlang distribution), U indicates a uniform service-time distribution at the transporter, n indicates the number of servers (transporters), K indicates the holding capacity of the periplasm (including adsorption to the inner surface of the outer membrane and the outer surface of the inner membrane), ∞ indicates that the source population of nutrients is unlimited, and RSS indicates that the nutrient molecules in the queue are processed in random order (random selection for service). Capacity of this system and hence average rate of gain are likely to depend on capsule and periplasm volume (proportional to r_0^3), but with the distal portions devalued because of their lower efficacy (Fig. 3). We suggest that these capabilities for dealing with rich nutrient pulses in an oligotrophic background have not been suspected before because they would be selected for in neither batch nor chemostat culture, where great lengths are taken to avoid local variations in nutrient concentration. Oligotrophs that appear maladapted to chronically low mean concentrations of nutrients in chemostats (Koch and Wang, 1982) may be well adapted to nature.

Environments not considered

We should make it clear that important microbial environments are excluded from our analysis. Because attachment allows relative motion of fluid past the attachment surface, it can enhance flux. Neighboring cells also can influence each other's environments and progeny can remain in close proximity. Enclosure either in pore spaces in sediments or in animal guts can lead to profit from release of free enzymes in solution, since the probability that the product of enzymatic reaction will return to the individual or a clone mate can rise well above the value indicated in Fig. 2. The laminar flow environments of pore waters, coupled with strong solute gradients make oxic sediments ideal sites for chemotaxis to play an important role in bacterial foraging. Again, however, cell-cell interactions are likely to be of great importance in determining fitness. Our review and essay covers only the plankton of large water bodies.

References

- Allen A.O., 1990. Probability, Statistics, and Queueing Theory, 2nd ed. Boston, Academic Press, Inc., 740 p.
- Atkins P.W., 1982. Physical Chemistry, 2nd ed. San Francisco, W.H. Freeman & Co., 1095 p.
- Azam F. and Ammerman J.W., 1984. Cycling of organic matter by bacterioplankton in pelagic marine ecosystems: microenvironmental considerations, 345–360. In : *Flows of Energy and Materials in Marine Ecosystems*, M.J.R. Fasham (ed.). New York, Plenum Press.
- Azam F. and Hodson R.E., 1981. Multiphasic kinetics for D-glucose uptake by assemblages of natural marine bacteria. *Mar. Ecol. Progr. Ser.*, **6**, 213-222.
- Azam F. and Smith D.C., 1991. Bacterial influence on the variability in the ocean's biogeochemical state: a mechanistic view, 213-236. In : *Particle Analysis in Oceanography*. S. Demers (ed.). Berlin, Springer-Verlag.
- Banse K., 1982. Cell volumes, maximal growth rates of unicellular algae and ciliates, and the role of ciliates in the marine pelagial. *Limnol. Oceanogr.*, **27**, 1059-1071.
- Batchelor G.K., 1979. Mass transfer from a particle suspended in fluid with a steady linear ambient velocity distribution. *J. Fluid Mech.*, **95**, 369-400.
- Batchelor G.K., 1980. Mass transfer from small particles suspended in turbulent fluid. *J. Fluid Mech.*, **98**, 609-623.
- Bělehrádek J., 1926. Protoplasmic viscosity as determined by a temperature coefficient of biological reactions. *Nature*, **118**, 478-480.
- Berg H.C., 1983. Random Walks in Biology. Princeton, NJ, Princeton Univ. Press, 142 p.
- Berg H.C. and Purcell E.M., 1977. Physics of chemoreception. *Biophys. J.*, **20**, 193-219.
- Best J., 1955. The inference of intracellular enzymatic properties for kinetics data obtained from living cells. *J. Cell. Comp. Physiol.*, **46**, 1-27.
- Bigg P.H., 1967. Density of water in S.I. units over the range 0-40°C. *Brit. J. Appl. Phys.*, **18**, 521-537.
- Bowen J.D. and Stolzenbach K.D., 1992. The concentration distribution near a continuous point source in steady homogeneous shear. *J. Fluid Mech.*, **256**, 95-110.
- Bowen J.D., Stolzenbach K.D. and Chisholm S.W., 1993. Simulating bacterial clustering around phytoplankton cells in a turbulent ocean. *Limnol. Oceanogr.*, **38**, 36-51.
- Canelli E. and Fuhs G.W., 1976. Effect of the sinking rate of two diatoms (*Thalassiosira* spp.) on uptake from low concentrations of phosphate. *J. Phycol.*, **12**, 93-99.
- Clift R., Grace J.R. and Weber M.E., 1978. Bubbles, Drops and Particles. New York, Academic Press, 380 p.
- Cohen D. and Parnas H., 1976. The optimal strategy for the metabolism of reserve materials in micro-organisms. *J. Theor. Biol.*, **56**, 19-55.

- Confer D.R. and Logan B.E., 1991. Increased bacterial uptake of macromolecular substrates with fluid shear. *Appl. Env. Microbiol.*, **57**, 3093-3100.
- Cowen J.P., 1992. Morphological study of marine bacterial capsules: Implications for marine aggregates. *Mar. Biol.*, **114**, 85-95.
- Cussler E.L., 1984. Diffusion: Mass Transfer in Fluid Systems. Cambridge, Cambridge Univ. Press.
- Delille D., Bouvy M. and Cahet G., 1988. Short-term variations of bacterioplankton in the Antarctic Zone: Terre Adelie area. *Microb. Ecol.*, **15**, 293-309.
- Deming J.W., 1993. Psychrophily in the deep sea. In : *Proc. 6th Int. Symp. on Microbial Ecology*, Barcelona, Sept. 6-11, 1992, Universitat de Barcelona, in press.
- Diamond J.M. and Karasov W.H., 1987. Adaptive regulation of intestinal nutrient transporters. *Proc. Nat. Acad. Sci. U.S.A.*, **84**, 2242-2245.
- Evans G.T. and Parslow J.S., 1985. A model of annual plankton cycles. *Biol. Oceanogr.*, **3**, 327-347.
- Fenchel T., 1984. Suspended bacteria as a food source, 301-315. In : *Flows of Energy and Materials in Marine Ecosystems*, M.J.R. Fasham (ed.). New York, Plenum Press.
- Frankel N.A. and Acrivos A., 1968. Heat and mass transfer from small spheres and cylinders freely suspended in shear flow. *Phys. Fluids*, **11**, 1913-1918.
- Gilliam J.F., 1989. Hunting by the hunted: Optimal prey selection by foragers under predation hazard, 797-819. In : *Behavioural Mechanisms of Diet Selection*, R.N. Hughes (ed.). Berlin, Springer-Verlag.
- Girard G., 1987. Section: Density, 6-38. In : *Recommended Reference Materials for the Realization of Physicochemical Properties*, K.N. Marsh (ed.). Oxford, Blackwell Scientific.
- Goldman J.C., 1984. Oceanic nutrient cycles, 137-170. In : *Flows of Energy and Materials in Marine Ecosystems*, M.J.R. Fasham (ed.). New York, Plenum Press.
- Hagström Å. and Larsson U., 1984. Diel and seasonal variation in growth rates of pelagic bacteria, 249-262. In : *Heterotrophic Activity in the Sea*, J.E. Hobbie and P.J. leB. Williams (eds.). New York, Plenum.
- Haight J.J. and Morita R.Y., 1966. Some physiological differences in *Vibrio marinus* grown at environmental and optimal temperatures. *Limnol. Oceanogr.*, **11**, 470-474.
- Hochachka P.W. and Somero G.W., 1984. Biochemical Adaptation. Princeton, N.J., Princeton Univ. Press, 537 p.
- Horvath C. and Engasser J.-M., 1974. External and internal diffusion in heterogeneous enzymes [sic.] systems. *Biotech. Bioeng.*, **16**, 909-923.
- Hudson R.J.M. and Morel F.M.M., 1993. Trace metal transport by marine microorganisms: implications of metal coordination kinetics. *Deep-Sea Res.*, **40**, 129-150.
- Huettel M. and Gust G., 1992. Solute release mechanisms from confined sediment cores in stirred benthic chambers and flume flows. *Mar. Ecol. Progr. Ser.*, **82**, 187-197.
- Jackson G.A., 1980. Phytoplankton growth and zooplankton grazing in oligotrophic oceans. *Nature*, **284**, 439-441.
- Jackson G.A., 1987. Physical and chemical properties of aquatic environments, 213-233. In : *Ecology of Microbial Communities*, M. Fletcher (ed.). Cambridge, Cambridge Univ. Press.
- Jenkinson I.R. and Wyatt T., 1992. Selection and control of Deborah numbers in plankton ecology. *J. Plankton Ecol.*, **14**, 1697-1721.
- Johnston A.M. and Raven J.A., 1992. Effect of aeration rates on growth rates and natural abundance ¹³C/¹⁴C ratio of *Phaeodactylum tricornutum*. *Mar. Ecol. Progr. Ser.*, **87**, 295-300.
- Jumars P.A., 1993. Concepts in Biological Oceanography: An Interdisciplinary Primer. New York, Oxford Univ. Press, 348 p.
- Jumars P.A., Penry D.L., Baross J.A., Perry M.J. and Frost B.W., 1989. Closing the microbial loop: Dissolved carbon pathway to heterotrophic bacteria from incomplete digestion and absorption in animals. *Deep-Sea Res.*, **36**, 483-495.
- Keeler K.H., 1985. Cost: benefit models of mutualism, 100-127. In : *The Biology of Mutualism*, D.H. Boucher (ed.). London, Croom Helm.
- Koch A.L., 1971. The adaptive response of *Escherichia coli* to a feast and famine existence. *Adv. Microb. Physiol.*, **6**, 147-217.
- Koch A.L., 1982. Multistep kinetics: Choice of models for the growth of bacteria. *J. Theor. Biol.*, **98**, 401-417.

- Koch A.L., 1985. The macroeconomics of bacterial growth, 1-42. In : *Bacteria in Their Natural Environments*, M. Fletcher and G.D. Floodgate (eds.). London, Academic Press.
- Koch A.L., 1990. Diffusion, the crucial process in many aspects of the biology of bacteria. *Adv. Microbial Ecol.*, **11**, 37-70.
- Koch A.L. and Coffman R., 1970. Diffusion, permeation, or enzyme limitation: a probe for the kinetics of enzyme induction. *Biotech. Bioeng.*, **12**, 651-677.
- Koch A.L. and Wang C.H., 1982. How close to the theoretical diffusion limit do bacterial uptake systems function? *Arch. Microbiol.*, **131**, 36-42.
- Korson L., Drost-Hansen W. and Millero F.J., 1969. Viscosity of water at various temperatures. *J. Phys. Chem.*, **73**, 34-39.
- Kottmeier S.T. and Sullivan C.W., 1988. Sea Ice Microbial Communities (SIMCO). 9. Effects of temperature and salinity on rates of metabolism and growth of autotrophs and heterotrophs. *Polar Biol.*, **8**, 293-304.
- Larsson U. and Hagström Å., 1982. Fractionated phytoplankton primary production, exudate release and bacterial production in a Baltic eutrophication gradient. *Mar. Biol.*, **67**, 57-70.
- Lazier J.R.N. and Mann K.H., 1989. Turbulence and diffusive layers around small organisms. *Deep-Sea Res.*, **36**, 1721-1733.
- Lehman J.T. and Scavia D., 1982. Microscale patchiness of nutrients in plankton communities. *Science*, **216**, 729-730.
- Levenspiel O., 1972. Chemical Reaction Engineering. New York, John Wiley & Sons, 578 p.
- Li W.K.W., Smith J.C. and Platt T., 1984. Temperature response of photosynthetic capacity and carboxylase activity in Arctic marine phytoplankton. *Mar. Ecol. Progr. Ser.*, **17**, 237-243.
- Li Y.-H. and Gregory S., 1974. Diffusion of ions in sea water and in deep-sea sediments. *Geochim. Cosmochim. Acta*, **38**, 703-714.
- Logan B.E. and Dettmer J.W., 1990. Increased mass transfer to microorganisms with fluid motion. *Biotech. Bioeng.*, **35**, 1135-1144.
- Logan B.E. and Hunt R.J., 1988. Bioflocculation as a microbial response to substrate limitations. *Biotech. Bioeng.*, **31**, 91-101.
- Logan B.E. and Kirchman, D.L., 1991. Uptake of dissolved organics by marine bacteria as a function of fluid motion. *Mar. Biol.*, **111**, 175-181.
- Maddock J.R. and Shapiro L., 1993. Polar location of the chemoreceptor complex in the *Escherichia coli* cell. *Science*, **259**, 1717-1723.
- Mann K.H. and Lazier J.R.N., 1991. Dynamics of Marine Ecosystems. Boston, Blackwell Scientific Publ., 466 p.
- McMeekin T.A., Olley J. and Ratkowsky D.A., 1988. Temperature effects on bacterial growth rates, 75-89. In : *Physiological Models in Microbiology*, M.J. Bazin and J.I. Prosser (eds.). Boca Raton, FL, CRC Press.
- Millero F.J., 1974. Seawater as a multicomponent electrolyte solution, 1-80. In : *The Sea*, Vol. 5. E.D. Goldberg (ed). New York, Wiley-Interscience.
- Millero F.J. and Poisson A., 1981. International one-atmosphere equation of state of seawater. *Deep-Sea Res.*, **28A**, 625-629.
- Millero F.J., Chen C.-T., Bradshaw A. and Schleicher K., 1980. A new high pressure equation of state for seawater. *Deep-Sea Res.*, **27A**, 255-264.
- Mitchell J.G., 1991. The influence of cell size on marine bacterial motility and energetics. *Microb. Ecol.*, **22**, 227-238.
- Morel F.M.M., 1987. Kinetics of nutrient uptake and growth in phytoplankton. *J. Phycol.*, **23**, 137-150.
- Morel F.M.M., Hudson R.J.M. and Price N.M., 1991. Limitation of productivity by trace metals in the sea. *Limnol. Oceanogr.*, **36**, 1742-1755.
- Neidhardt F.C., Ingraham J.L. and Schaechter M., 1990. Physiology of the Bacterial Cell: A Molecular Approach. Sunderland, MA., 506 p.
- Nikaido H. and Saier M.H. Jr., 1992. Transport proteins in bacteria: Common themes in their design. *Science*, **258**, 936-942.
- Oelkers E.H., 1991. Calculation of diffusion coefficients for aqueous organic species at temperatures from 0 to 250°C. *Geochim. Cosmochim. Acta*, **55**, 3515-3529.

- Oelkers E.H. and Helgeson H.C., 1988. Calculation of the thermodynamic and transport properties of aqueous species at high pressures and temperatures: Aqueous tracer diffusion coefficients of ions to 1000°C and 5 kb. *Geochim. Cosmochim. Acta*, **52**, 63-85.
- Parnas H. and Cohen D., 1976. The optimal strategy for the metabolism of reserve materials in micro-organisms. *J. Theor. Biol.*, **56**, 19-55.
- Pasciak W.J. and Gavis J., 1974. Transport limitation of nutrient uptake in phytoplankton. *Limnol. Oceanogr.*, **6**, 881-888.
- Pasciak W.J. and Gavis J., 1975. Transport limited nutrient uptake rates in *Dytilum brighwellii*. *Limnol. Oceanogr.*, **20**, 604-617.
- Plante C.J., Jumars P.A. and Baross J.A. 1990. Digestive associations between marine detritivores and bacteria. *Ann. Rev. Ecol. Syst.*, **21**, 93-127.
- Pomeroy L.R., 1974. The ocean's food web, a changing paradigm. *BioSci.*, **24**, 499-504.
- Pomeroy L.R. and Deibel D., 1986. Temperature regulation of bacterial activity during the spring bloom in Newfoundland coastal waters. *Science*, **233**, 359-361.
- Pomeroy L.R., Macko S.A., Ostrom P.H. and Dunphy J., 1990. The microbial food web in Arctic seawater: concentration of dissolved free amino acids and bacterial abundance and activity in the Arctic Ocean and in Resolute Passage. *Mar. Ecol. Progr. Ser.*, **61**, 31-40.
- Pomeroy L.R., Wiebe W.J., Deibel D., Thompson R.J., Rowe G.T. and Pakulski J.D., 1991. Bacterial responses to temperature and substrate concentration during the Newfoundland spring bloom. *Mar. Ecol. Progr. Ser.*, **75**, 143-159.
- Powell E.O., 1967. Growth rate of microorganisms as a function of substrate concentration, 34-55. In : *Microbial Physiology and Continuous Culture*, E.O. Powell, C.G.T. Evans, R.E. Strange and D.W. Tempest (eds.). London, Her Majesty's Stationery Office.
- Pugsley A.P., 1993. The complete general secretory pathway in gram-negative bacteria. *Microb. Rev.*, **57**, 50-108.
- Purcell E.M., 1978. The effect of fluid motions on the absorption of molecules by suspended particles. *J. Fluid Mech.*, **84**, 551-559.
- Ratkowsky D.A., Olley J., McMeekin T.A. and Ball A., 1982. Relationship between growth rate and temperature of bacterial cultures. *J. Bacteriol.*, **149**, 1-5.
- Ratkowsky D.A., Lowry R.K., McMeekin T.A., Stokes K.N. and Chandler R.E., 1983. Model for bacterial culture growth throughout the entire biokinetic temperature range. *J. Bacteriol.*, **154**, 1222-1226.
- Riebesell U., Wolf-Gladrow D.A. and Smetacek V., 1993. Carbon dioxide limitation of marine phytoplankton growth rates. *Nature*, **361**, 249-251.
- Saffman P.G. and J.S. Turner, 1956. On the collision of drops in turbulent clouds. *J. Fluid Mech.*, **1**, 16-30.
- Scavia D. and Laird G.A., 1987. Bacterioplankton in Lake Michigan: dynamics, controls, and significance to carbon flux. *Limnol. Oceanogr.*, **32**, 1017-1033.
- Segel I.H., 1975. *Enzyme Kinetics: Behavior and Analysis of Rapid Equilibrium and Steady-State Enzyme Systems*. New York, Wiley-Interscience, 957 p.
- Sengers J.V. and Watson J.T.R., 1986. Improved international formulations for the viscosity and thermal conductivity of water substance. *J. Phys. Chem. Ref. Data*, **15**, 1291-1314.
- Shimeta J., 1993. Diffusional encounter of submicrometer particles and small cells by suspension feeders. *Limnol. Oceanogr.*, **38**, 456-465.
- Shimeta J. and Jumars P.A., 1991. Physical mechanisms and rates of particle capture by suspension feeders. *Oceanogr. Mar. Biol. Ann. Rev.*, **29**, 191-257.
- Sommer U., 1989. Maximal growth rates of Antarctic phytoplankton: Only weak dependence on cell size. *Limnol. Oceanogr.*, **34**, 1109-1112.
- Stephens D.W. and Krebs J.R., 1986. *Foraging Theory*. Princeton, NJ, Princeton Univ. Press, 247 p.
- Suttle C.A., Stockner J.G. and Harrison P.J., 1987. Effects of nutrient pulses on community structure and cell size of a freshwater phytoplankton assemblage in culture. *Can J. Fish. Aquat. Sci.*, **44**, 1768-1774.
- Suttle C.A., Stockner J.G., Shortreed K.S. and Harrison P.J., 1988. Time-courses of size-fractionated phosphate uptake: are larger cells better competitors for pulses of phosphate than small cells. *Oecologia*, **74**, 571-576.

- Thingstad T.F. and Martinussen I., 1991. Are bacteria active in the cold pelagic ecosystem of the Barents Sea? *Polar Res.*, **10**, 256-266.
- UNESCO, 1981. Background papers and supporting data on the international equation of state of seawater 1980. *Unesco Technical Papers in Marine Science*, **38**, 1-191.
- Waite B.A. and Stewart J.D., 1993. An idealized dynamical model of simple diffusional interactions between macromolecules and surfaces. *Math. Biosci.*, **114**, 173-213.
- Wikner J. and Hagström Å., 1991. Annual study of bacterioplankton community dynamics. *Limnol. Oceanogr.*, **36**, 1313-1324.

Appendix

Densities and Dynamic Viscosities of Fresh and Salt Water

For pure water (designated by the subscript fw for fresh water), an accurate prediction of dynamic viscosity (< 1% error over the full range from 0–40°C; Korson *et al.*, 1969) results from the equation:

$$\log_{10} \mu_{fw} = \frac{-157.095 - 3.09695T - 0.001827T^2}{89.93 + T} \quad (A1)$$

where T is temperature in °C and μ_{fw} is in units of poise ($\text{g cm}^{-1} \text{s}^{-1}$). For calculational convenience, we have converted Korson *et al.*'s (1969) original equation to cgs units and from natural logarithms to logarithms in base ten. (To obtain SI units of Pa s for this dynamic viscosity and others considered below, multiply the final viscosity by 0.1 or subtract 1.0 from the right side of Eq. A1.) Now accepted internationally for pure water is a much more complex interpolating formula with 19 coefficients (Sengers and Watson, 1986) that should be used instead when great accuracy and precision are needed, especially above 40°C. Eq. A1 slightly underestimates dynamic viscosity at 0°C to be 0.01791, compared to the 0.01793 given by Sengers and Watson (1986).

Dynamic viscosity of seawater is usually calculated from the density of seawater, ρ_{sw} , which in turn is usually calculated from the density of fresh water, ρ_{fw} , both in units of g cm^{-3} (Bigg, 1967):

$$\rho_{fw} = 0.999842594 + 6.793952 \times 10^{-5}T - 9.09529 \times 10^{-6}T^2 + 1.001685 \times 10^{-7}T^3 - 1.120083 \times 10^{-9}T^4 + 6.536332 \times 10^{-12}T^5 \quad (A2)$$

(To obtain SI units of kg m^{-3} for density, multiply the result by 10^3 .) Potential improvements may result from further evaluations of isotopic composition of natural seawater and agreement regarding the correspondence between modern temperature scales and historical measurements, but this interpolation equation retains international acceptance (Girard, 1987). The density of seawater, in turn, is calculated as (Millero and Poisson, 1981):

$$\rho_{sw} = \rho_{fw} + AS + BS^{\frac{3}{2}} + CS^2 \quad (A3)$$

where S is salinity (‰). The terms, A , B and C are defined as follows:

$$A = 8.24493 \times 10^{-4} - 4.0899 \times 10^{-6}T + 7.6438 \times 10^{-8}T^2 - 8.2467 \times 10^{-10}T^3 + 5.3875 \times 10^{-12}T^4 \quad (A4)$$

$$B = -5.72466 \times 10^{-6} + 1.0227 \times 10^{-7}T - 1.6546 \times 10^{-9}T^2; \text{ and,} \quad (A5)$$

$$C = 4.8314 \times 10^{-7} \quad (\text{A6})$$

Above atmospheric pressure, further terms are needed (Millero *et al.*, 1980). In either case one may find the added information in UNESCO (1981) helpful in evaluating fit of these equations to data and in checking the output of implementations.

Finally, then, dynamic viscosity of seawater (μ_{sw} , poise) can be calculated as (Millero, 1974):

$$\mu_{sw} = \mu_{fw} (1 + E\sqrt{Cl_v} + FCl_v), \text{ where} \quad (\text{A7})$$

$$E = 1.068 \times 10^{-4} + 5.185 \times 10^{-5}T, \quad (\text{A8})$$

$$F = 2.591 \times 10^{-3} + 3.3 \times 10^{-5}T \text{ and} \quad (\text{A9})$$

$$Cl_v = \frac{\rho_{sw} S}{1.80655} \quad (\text{A10})$$

Here Cl_v is the volume chlorinity. This set of equations (A7-A10) has been neither subjected to as much scrutiny as the previous equations for viscosity of fresh water or the densities of fresh and salt water nor approved by international consensus. Clear shortcomings are that it has not been tested against data below 0°C and that the multipliers E and F have been evaluated only at 5 and 25°C. Note that temperature dependence of Eq. A7 is not transparent from the factors E and F alone, since μ_{fw} also depends upon temperature as does Cl_v through its dependence on ρ_{sw} .

